Western Graduate&PostdoctoralStudies

Western University
Scholarship@Western

Electronic Thesis and Dissertation Repository

1-6-2017 12:00 AM

Effect of L-Ascorbic Acid and All-trans Retinoic Acid on Smooth Muscle Cells Cultured on PCL Scaffolds

Brandon Chaffay, *The University of Western Ontario*

Supervisor: Dr. Kibret Mequanint, *The University of Western Ontario*

A thesis submitted in partial fulfillment of the requirements for the Master of Engineering Science degree in Chemical and Biochemical Engineering

© Brandon Chaffay 2017

Follow this and additional works at: https://ir.lib.uwo.ca/etd

Part of the Biological Engineering Commons, and the Biomaterials Commons

Recommended Citation

Chaffay, Brandon, "Effect of L-Ascorbic Acid and All-trans Retinoic Acid on Smooth Muscle Cells Cultured on PCL Scaffolds" (2017). *Electronic Thesis and Dissertation Repository*. 4369.
https://ir.lib.uwo.ca/etd/4369

This Dissertation/Thesis is brought to you for free and open access by Scholarship@Western. It has been accepted for inclusion in Electronic Thesis and Dissertation Repository by an authorized administrator of Scholarship@Western. For more information, please contact wlswadmin@uwo.ca.

Abstract

The aim of vascular tissue engineering (VTE) is to fabricate tissues that are both mechanically and biologically competent similar to the native vessel they are intended to replace. To this end, the incorporation of sufficient extracellular matrix elastin and collagen is important. The objective of this thesis work was to evaluate the effect of two biochemical factors, L-ascorbic acid (AA) and all-*trans* retinoic acid (atRA), on elastin synthesis when coronary artery smooth muscle cells were cultured on 3D polycaprolactone (PCL) scaffolds. First, porous PCL scaffolds were fabricated using a solvent casting and particulate leaching approach. The effect of different solvents (ethyl acetate, chloroform and tetrahydrofuran) and PCL concentration on the morphology and porosity of the resulting scaffolds were studied. The best scaffolds (based on SEM and micro-CT analyses) were fabricated from 30% w/w PCL in ethyl acetate. Second, smooth muscle cells were cultured on these scaffolds to evaluate elastin synthesis. It was found that concurrent addition of AA and atRA in both 2-D and 3-D cultures suppressed elastin protein expression compared with atRA alone. To overcome this effect, sequential biochemical factors addition was tested. The results demonstrated that sequential but not concurrent addition of biochemical agents promoted tropoelastin synthesis. This study suggested the importance of biochemical factor addition strategy to engineer a viable vascular tissue.

Keywords: vascular tissue engineering, vascular smooth muscle cells, elastin, all-*trans* retinoic acid, L-ascorbic acid, PCL scaffolds.

Acknowledgements

I am sincerely grateful to my supervisor, Dr. Kibret Mequanint, who has guided me these past years. While the learning curve was steep, Dr. Mequanint was always there to ensure that I stayed on the right track and focused on the big picture. His continued mentorship made me to be a well-rounded and independent student. I would like to thank Dr. Shigang Lin and Dr. Kalin Penev, both of whom provided invaluable advice and were always available for a quick discussion about the field and ways to constantly improve. I am very appreciative of Dibakar Mondal for his assistance with the micro-CT data reconstruction. Most importantly, I am thankful for having an understanding family that has been by my side and supported me unconditionally.

Table of Contents

Abstract ii
Acknowledgements iii
List of Tables vii
List of Figures viii
List of Abbreviations xi

Chapter 1 - Introduction 1
1.1 Overview 1
1.2 Thesis Outline 2

Chapter 2 – Literature Review 4
2.1 Vasculature Organization and Function 4
2.1.1 Circulation Anatomy 4
2.1.2 Arterial Circulation: Structural and Histological Detail 5
2.1.3 Arterial Circulation: Extracellular Matrix (ECM) Proteins and Associated Mechanical Properties 6
2.2 Coronary Arterial Circulation 11
2.3 Coronary Artery Disease (CAD) 12
2.4 Therapeutic Interventions for CAD 14
2.5 Vascular Tissue Engineering (VTE) 16
2.5.1 Overview 16
2.5.2 Cell Source 17
2.5.3 Scaffolds 19
2.5.4 Bioreactors 22
2.6 Small-Diameter VTE: Challenges and Potential Solutions 22
2.7 Vascular Smooth Muscle Cell (vSMC) Culture 24
2.7.1 vSMC Phenotype 24
2.7.2 vSMC Response to Microenvironments: 2-D vs. 3-D Culture 25
2.8 Retinoids 27
2.8.1 Overview 27
2.8.2 atRA Impact on vSMC Phenotype 29
2.8.3 atRA Impact on Elastin Expression 30

2.8.4 atRA in Combination with Ascorbic Acid: Impact on Elastin 31
2.9 Study Rationale and Objectives 31

Chapter 3 – Materials and Methods 33
3.1 Materials 33
3.2 Methods 34
3.2.1 Scaffold Fabrication *via* Solvent Casting and Particulate Leaching (SCPL) ... 34
3.2.2 Scaffold Characterization 36
3.2.3 Cell Culture Conditions 36
3.2.4 Scaffold Preparation for Cell Culture 37
3.2.5 2-D and 3-D Culture 37
3.2.6 Cell Viability and Proliferation Assays 38
3.2.7 Immunofluorescence Staining and Confocal Imaging in 3-D Culture 39
3.2.8 RNA Isolation and Gene Expression Studies Using Real-Time PCR (qPCR) Analysis 39
3.2.9 Protein Analysis Using Western Blotting 40
3.2.10 Statistical Analysis 41

Chapter 4 – Results and Discussion 42
4.1 Scaffold Characterization 42
4.1.1 General Observations during Scaffold Fabrication 42
4.1.2 Scanning Electron Microscopy (SEM) 44
4.1.3 Micro-CT analysis of 3-D Scaffolds 48
4.2 Assessing Cell Viability and Proliferation 50
4.3 The Effect of atRA on Cultured Smooth Muscle Cells 54
4.3.1 Cell Morphological Response to atRA Treatment 54
4.3.2 The effect of atRA Concentration on Elastin Gene Expression 58
4.4 The Effect of AA and atRA Combination on Tropoelastin Synthesis 59
4.5 Comparative Study of Elastin Synthesis in 2D Plates and 3D PCL Scaffolds 62
4.5.1 Spatial Effects on Elastin Synthesis 62
4.5.2 Combinational Approach to Rescue Elastin Expression in 3-D Culture 64
4.5.3 The Effect of Biochemical Factors on α-SMA Expression 66

Chapter 5 – Conclusions and Future Directions 69
5.1 Conclusions 69
5.2 Future Directions 71

6. References.....72

Appendix: Copyright Permission..... 88
Curriculum Vitae 87

List of Tables

Table 4.1: Variables considered for solvent casting particulate leaching (SCPL) process to fabricate PCL Scaffolds. 43

Table 4.2: Micro-CT analysis of 3-D PCL scaffolds at varying w/w concentrations dissolved in either $CHCl_3$ or EtOAc. Two different scaffolds were fabricated and three random measurements were taken for each scaffold (n = 6). 49

List of Figures

Figure 2.1: A. Longitudinal section of an artery indicating the exposed vessel wall layers. B. Histological cross-section indicating extensive lamellar elastin distribution within the medial layer.[11] Used with permission from the Publisher. 6

Figure 2.2: Nonlinear mechanical behavior of an artery. A: average circumferential stress versus stretch ratio. B: circumferential incremental elastic modulus (Einc) versus stretch ratio. Einc was calculated by determining the local slope of the stress-stretch ratio relationship in Fig. A. Data shown is for adult mouse aorta.[5] Used with permission from the Publisher..... 8

Figure 2.3: A. Assembly process of elastic fibers beginning at tropoelastin secretion and association with the cellular membrane where cross-linking occurs by lysyl oxidase. B. Silver stain (van Gieson) indicating that elastin is most evident within the medial layer of the vessel wall.[25] Used with permission from the Publisher. 10

Figure 2.4: Process description for vascular tissue engineering (VTE). The overall approach is to harvest cells from patients, expand them in culture and seed them to a 3-D scaffold for maturation and remodeling in a bioreactor. 17

Figure 2.5: Intracellular effects of atRA. After being transported through the plasma by a protein carrier, albumin, atRA translocates across the membrane and associates with the CRABPs that allow nuclear translocation and subsequent transcriptional effects.[113] Used with permission from the Publisher 28

Figure 3.1: Solvent casting and particulate leaching apparatus. The digital images shown are the tubular scaffolds fabricated using the apparatus. 35

Figure 4.1: Ablumenal SEM images of 20-30% w/w PCL scaffolds fabricated using SCPL. PCL was dissolved in CHCl3 (A-C), EtOAc (D-F) and THF (G-I). Scale bar represents 500 μm. 45

Figure 4.2: Lumenal SEM images of 20-30% w/w PCL scaffolds fabricated using SCPL. PCL dissolved in CHCl3 (A, B), EtOAc (C, D) and THF (E, F). Scale bar represents 1000 μm. 46

Figure 4.3: SEM cross-sectional images of 20-30% w/w PCL tubular scaffolds fabricated using SCPL. PCL was dissolved in CHCl3 (A-C); EtOAc (D-F) and THF (G-I). Scale bar represents 500 μm. 48

Figure 4.4: Micro-CT images of PCL scaffolds fabricated by dissolving in either CHCl3 or EtOAc at varying w/w concentrations. A-C. PCL dissolved in CHCl3. D-F. PCL dissolved in EtOAc. The images are specific volume elements representing the cross-section within the scaffolds. The white within the image represents PCL and the grey regions represent the pores..... 49

Figure 4.5: MTT assays of NIH-3T3 fibroblasts or hcSMCs on 20%, 25%, or 30% w/w PCL scaffolds dissolved in EtOAc. A: Viability of NIH-3T3 fibroblasts assessed at day 4 and 7. B: Viability of hcSMCs assessed at day 4 and 7. Significance: $p<0.05$ (*)..... 52

Figure 4.6: DNA quantification of hcSMCs seeded onto 30% w/w PCL scaffolds at days 4 and 7. Significance: $p<0.05$ (*), $p<0.01$ (**), $p<0.001$ (***). 54

Figure 4.7: Confocal images of hcSMCs seeded onto porous 3-D polyurethane scaffolds and exposed to 100 μM of atRA. Confocal images were taken after 4 and 7 days of culture. Scale bar represents 200 μm. Staining: F-actin (green) and DAPI (red). 56

Figure 4.8: Confocal images of hcSMCs seeded on a porous 3-D polyurethane scaffold with or without fibronectin pre-treatment and 150 μM atRA. Cells were cultured for 14 days before fixation and confocal imaging. Scale bar represents 200 μm. Staining: F-actin (green) and DAPI (red). 57

Figure 4.9: The effect of atRA concentration on tropoelastin gene expression in hcSMCs cultured on 2D plates for 4 days. 10 μM atRA produced the highest tropoelastin fold increase and was utilized for subsequent experiments. Significance: $p<0.05$ (*) was observed for 10 μM of atRA compared to the untreated control (C) and 0.1 and 1 μM of atRA. 59

Figure 4.10: Time-course evaluation tropoelastin synthesis (as determined by Western blot) isolated from whole-cell lysates of hcSMCs in response to various biochemical factor treatments. Data are normalized to GAPDH and a control without biochemical factor treatment. Significance: $p<0.05$ (*) was observed as indicated in the graph. 61

Figure 4.11: qPCR assessing tropoelastin transcription in hcSMCs at 48, 72, and 96 hours comparing a combination of AA and atRA to a non-treated control, both normalized to GAPDH. Significance: $p<0.05$ (*) was observed for the combination treatment relative to the untreated control at the 48-hour time point. NS: Not significant. 62

Figure 4.12: Western blotting of whole-cell lysates of hcSMCs assessing for tropoelastin expression in response to biochemical factor treatment in 2D culture plates (A) and 3D PCL scaffolds (B). Data was normalized to GAPDH and a non-treated control. Significance: $p<0.05$ (*). 63

Figure 4.13: Elastin expression assessed by Western blotting of whole-cell lysates of hcSMCs after sequential non-overlapping factor exposure for different times. The schematic of the experimental design is shown in A where cells were cultured either without treatment (control), 6 days of AA treatment, 5 days AA followed by 1 day atRA treatment or 3 days AA followed by 3 days atRA treatment. Cells were harvested on the 7^{th} day for protein extraction and Western blotting. Significance: $p<0.05$ (*) was observed for 3 days of atRA rescue compared to AA alone. 65

Figure 4.14: Western blotting of whole-cell lysates of hcSMCs assessing for α-SMA normalized to GAPDH at day 4 and day 7 cultures for 2D cultures (A, B) and 3D cultures (C, D). Significance: $p<0.05$ (*). 67

List of Abbreviations

2-D	Two dimensional
3-D	Three-dimensional
α-SMA	Smooth muscle alpha actin
atRA	all-*trans* Retinoic Acid
BSA	Bovine serum albumin
bFGF	Basic fibroblast growth factor
CAD	Coronary artery disease
CVD	Cardiovascular disease
DMEM	Dulbecco's modified eagle's medium
EC	Endothelial cell
ECM	Extracellular matrix
EtOAc	Ethyl Acetate
FBS	Fetal bovine serum
GAPDH	Glyceraldehyde 3-phosphate dehydrogenase
hcSMC	Human coronary artery smooth muscle cell
LAD	Left anterior descending
L-AA	L-Ascorbic Acid
LCA	Left coronary artery
LDL	Low-density lipoprotein
LOX	Lysyl oxidase
NO	Nitric oxide
qPCR	Real-time PCR
PCL	ε-Polycaprolactone
PBS	Phosphate buffered saline
PAGE	Polyacrylamide gel electrophoresis
PCR	Polymerase chain reaction
RCA	Right coronary artery
SCPL	Solvent casting and particulate leaching
SDS	Sodium dodecyl sulfate
SEM	Scanning electron microscopy
SMC	Smooth muscle cell
THF	Tetrahydrofuran
TEBV	Tissue-engineered blood vessel
vSMC	Vascular smooth muscle cell
VTE	Vascular tissue engineering

Chapter 1 - Introduction

1.1 Overview

Despite significant progress made in intervention outcomes, cardiovascular disease (CVD) represents the leading cause of death worldwide. Diseases impacting the small diameter vasculature, such as the vessels servicing the coronary circulation, are becoming the leading cause of mortality for all of CVD [1]. Alarmingly, these trends are predicted to increase in the future, likely attributed to an aging population prone to making poor health decisions. Prophylactic measures to reduce the incidence of CVD have not been effective due to compliance issues.[2] For replacement of the diseased coronary arteries, autologous vessels such as the great saphenous vein or internal thoracic artery are the most viable options yet the likely presence of co-morbidities or removal from previous harvests indicate that other options are required. While it is possible to utilize allografts or xenografts, there are significant immune-mediated issues that arise that decrease the patency of these grafts. As such, there is need for the development of a therapeutically viable and highly patent small-diameter graft replacement. This can be accomplished through vascular tissue engineering (VTE) that aims to mimic a native vessel through synthetic fabrication methods. However, the success of such designs relies on matching the mechanical properties to that of the native vessels.[3] As collagen and elastin are the two main proteins that endow the native vessels with their mechanical properties, it is important to understand their expression in order for enhancement to occur *in vitro*.

While collagen can be increased *in vitro* through L-Ascorbic Acid (AA) addition, a main challenge of VTE is an inability to understand and promote elastogenesis. Elastin provides resiliency to the arteries and allows for the accommodation of cyclic loading during the cardiac cycle. It is thought that elastogenic factors, that aid in stimulating the process, represent viable avenues to explore. One such factor is all-trans retinoic acid (atRA) that is a derivative of vitamin A and essential during embryonic development. atRA has been shown to promote the expression of elastin in 2-D cultures. Additionally, atRA is suggested to have significant phenotypic control over vascular smooth muscle cells (vSMCs) whereby a contractile state is produced that is non-proliferative. Thus, atRA appears to be an ideal candidate for investigation as it can increase elastin while concurrently mitigating the risk of restenosis usually seen with surgical interventions.[4] That said, few studies have investigated the combination of AA and atRA on 3-D scaffolds and those that did utilize long end-points and failed to assess elastogenesis acutely compared to either factor alone.

1.2 Thesis Outline

The thesis contains five chapters that are based on investigations pertaining to the interaction of hcSMCs with 2-D and 3-D substrates and the fabrication process of 3-D scaffolds. Chapter 2 introduces the relevant literature of the vasculature anatomy, vascular disease progression, therapeutic options to treat the pathologies, followed by the need for vascular tissue engineering and options to augment elastogenesis. The motivation and objectives of this study are discussed at the end of the chapter. Chapter 3 introduces the materials and methods and outlines the techniques utilized. Chapter 4 discusses the major

findings and results from the work. Chapter 5 comments on the future directions of the work and potential implications of the findings.

Chapter 2 – Literature Review

2.1 Vasculature Organization and Function

2.1.1 Circulation Anatomy

Blood vessels are hollow tubes that act as conduits for the cardiac output of the heart, allowing for systemic tissue perfusion with an oxygenated blood flow while facilitating the return of deoxygenated blood to the heart. The contraction of the left ventricle of the heart allows for the distribution of oxygenated blood systemically *via* the aorta, the initial segment of the arterial circulation. Distal to the aorta, numerous branches and bifurcations occur. Each newly created continuous segment is associated with an alternative lumenal diameter and deviation in the underlying structural detail of the vessel wall which imparts specific functionality.[5] The aorta transitions to smaller elastic then more muscular arteries which give rise to numerous arterioles and ultimately the capillaries.[5] The aorta acts as a Windkessel vessel, attempting to limit pulsatile blood flow in the periphery by dampening pulse pressure as it possesses relatively higher compliance than other derivatives in the arterial system.[6] The smaller arteries and the arterioles are more resistive in nature and thus have a larger impact on the maintenance of mean arterial pressure and control of distal flow. As the transition to arterioles occurs, there is a slight increase in the mean surface area of the vessels that reaches a maximum at the capillaries, which have the slowest flow velocity. Capillaries have the ideal hemodynamic characteristics for gas exchange and filtration or absorption due to their small wall thickness.[7] The capillaries converge after gas-exchange occurs at their proximal ends and become venules more distally, the first structure of the venous circulation. Most venules merge into smaller and then larger veins

that drain into the inferior or superior vena cava and back into the right atrium of the heart. Abnormalities in any section of this closed system will compromise downstream tissue perfusion and thus organ function.

2.1.2 Arterial Circulation: Structural and Histological Detail

The arterial wall is a tri-layered laminar structure consisting of the tunica intima, the tunica media, and the tunica adventitia.[5] Along the arterial tree, the composition of the arteries varies and similar, yet variant, stress-strain curves are observed.[8] Numerous studies have shown that the stress-strain curves will range from elastic to viscoelastic more distally with a continuum between these points.[5, 8, 9] The proceeding text describes the general features of an elastic or a more proximal muscular artery to which Figure 2.1 provides an overview of the arterial wall layers and underlying histological detail in cross-section.

The tunica intima is the innermost layer of the vessel wall that is exposed to the blood flow. It is composed of a mono-layer lining of endothelial cells (ECs) upon a basement membrane with a sub-endothelial matrix consisting of loose connective tissue, myointimal cells, fibroblasts, and extra-cellular constituents. Deep to the tunica intima lies the tunica media, a muscular layer consisting of circumferentially orientated smooth muscle cells (SMCs) and interspersed extra-cellular matrix fibers in a lamellar organization. The junction between the tunica media and overlying tunica intima is delineated by an internal elastic lamina, which assists in volume accommodation during the cardiac cycle and may have a role in SMC migration from the medial layer.[10] An external elastic lamina lies deeper and marks the junction between the overlying tunica media and the tunica

adventitia. The latter layer is more connective tissue in nature with fibroblasts in addition to collagenous fibers orientated longitudinally.

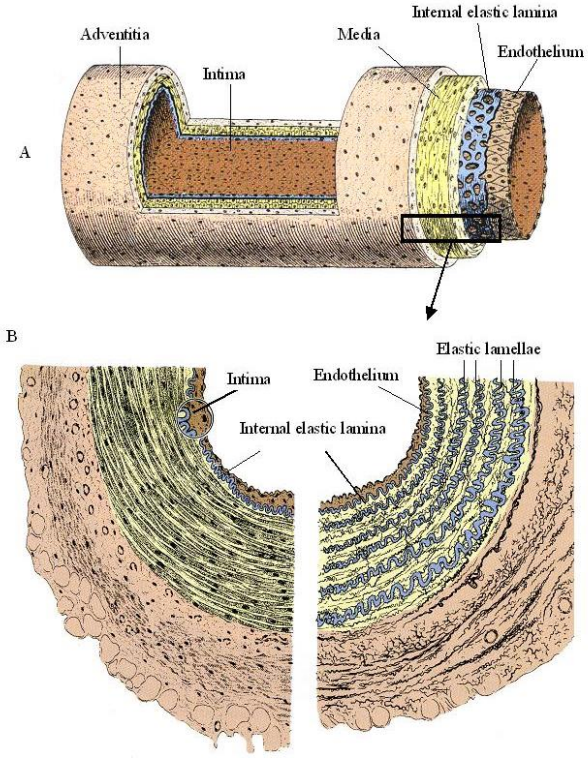

Figure 2.1: A. Longitudinal section of an artery indicating the exposed vessel wall layers. B. Histological cross-section indicating extensive lamellar elastin distribution within the medial layer.[11] Used with permission from the Publisher.

2.1.3 Arterial Circulation: Extracellular Matrix (ECM) Proteins and Associated Mechanical Properties

Compared with the highly compliant venous circulation, arteries have significantly higher elasticity, reversible recoil, and resilience at low strains.[5] These properties allow the arterial circulation to act as a pressure reservoir, to ensure that blood flows distally especially during diastole. However, the mechanical properties vary during alternative loading conditions and relate to the composite nature of arteries facilitating anisotropic mechanical responses. The classical arterial stress-strain relationship is a non-linear J-shaped curve possessing a low stiffness at low strains while transitioning exponentially to

a stiffer material at higher strains as shown in Figure 2.2.[5, 12] As such, blood vessels do not possess simple elastic properties, as non-linearity is observed when distended. These mechanical characteristics are due to numerous extracellular components produced by the cells within the vessel layers that collectively comprise the ECM. Specifically, these mechanical characteristics are due to components mainly within the medial layer, especially collagen and elastin.[5]

Collagen is a stiff, extracellular protein, possessing a high tensile strength of approximately 1.0×10^9 N/m^2, whose concentration is highest in the tunica adventitia.[13] In the unloaded condition, collagen assumes a "crimped" state yet when load is applied, additional collagen fibers will assume a greater proportion of the load-bearing and re-align in the direction of the applied stress.[14, 15] It was believed that the load-bearing ability of collagen in the medial layer begins at higher stresses until recently whereby Chow *et al*. [16] proposed that medial collagen may be engaged from the onset of strain. Yet, it is the recruitment of additional load-bearing in parallel with the high tensile strength of collagen that makes the protein an ideal structural support for protection against aneurysmal development and the potential for vessel wall rupture, as the artery becomes stiffer as the strain increases. However, collagen itself does not impart elasticity and it is elastin, an amorphous constituent within the ECM, that provides this mechanical property.

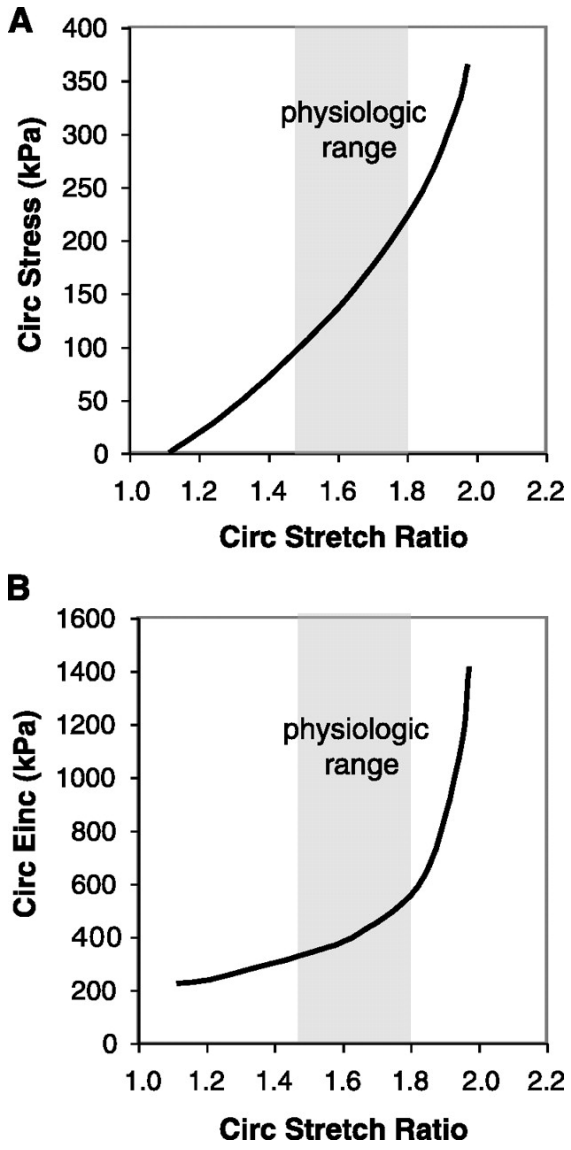

Figure 2.2: Nonlinear mechanical behavior of an artery. A: average circumferential stress versus stretch ratio. B: circumferential incremental elastic modulus (Einc) versus stretch ratio. Einc was calculated by determining the local slope of the stress-stretch ratio relationship in Fig. A. Data shown is for adult mouse aorta.[5] Used with permission from the Publisher.

Elastin exists within a composite of numerous ECM proteins that collectively are termed as elastic fibers.[17] Approximately 90% of the elastic fibers have been shown to be derived from elastin.[18] Intracellularly, elastin is transcribed as a 60-70 kDa tropoelastin precursor that contains numerous hydrophobic domains.[17] The transcriptional process is

developmentally regulated, with highest activity during late fetal and early neonatal period with minimal activity in adulthood due to post-transcriptional mechanisms at the downstream developmental stages.[19, 20]Additional segmental regulation occurs during these periods with the tissue-expression of elastin mainly being restricted to areas that undergo repetitive stresses.[21] When translated and excreted from the cell, tropoelastin becomes cross-linked at the cellular membrane by lysyl oxidase and the newly cross-linked structure is termed as elastin.[17] The aggregation is aided by the numerous hydrophobic domains which facilitate coacervation of the elastin subunits and promote the formation of strong desmosine and isodesmosine cross-links that provide the protein with its mechanical properties.[17, 22] The aggregates transfer to pre-existing micro-fibrils within the extra-cellular space, whereby the major component of the micro-fibrils, fibrillin-1, serves as a scaffold for elastin deposition.[17, 23] The assembling of the composite continues to increase in size as the elastin coalesces. The assembly process of tropoelastin to elastin and interaction with the pre-existing micro-fibrils is shown in Figure 2.3.

While elastin possesses a low tensile strength of approximately 4.6×10^5 N/m^2, it functions best to provide high resilience to the artery with a contributory low stiffness.[13] Chow *et al.*[24] have demonstrated that maximal elastin engagement within the medial layer is reached at approximately 20% strain. Elastin is engaged at these low strains to allow for slight distensibility of the arterial wall to accommodate increases in blood volume during the cardiac cycle.

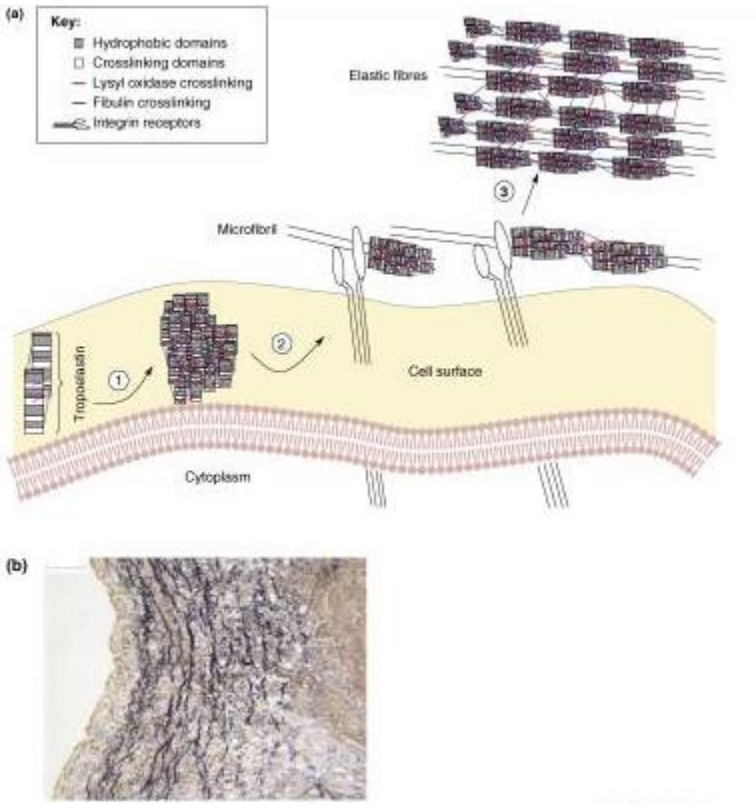

Figure 2.3: A. Assembly process of elastic fibers beginning at tropoelastin secretion and association with the cellular membrane where cross-linking occurs by lysyl oxidase. B. Silver stain (van Gieson) indicating that elastin is most evident within the medial layer of the vessel wall.[25] Used with permission from the Publisher.

As mentioned earlier, the medial layer contains numerous SMCs in a lamellar organization interlaced with elastic fibers. The geometry of the tunica media aids in accommodating the cyclic circumferential strain due to the cardiac cycle. The developing wall stress during systole is uniformly distributed on the vessel wall due to the residual stress being greater than zero and studies have suggested that this effect can be mainly attributed to elastin within the medial layer.[26, 27]At low stresses, the elastic lamellae become more aligned and taut yet the collagen alignment is more gradual and activated at much higher stresses. However, during disease states, the underlying structure will be significantly altered. Various pathologies, including age-induced degeneration, atherosclerosis, and

hypertension can influence the integrity of the fibers and alternative mechanical properties will be observed.[15, 28]

2.2 Coronary Arterial Circulation

The coronary arterial circulation is a collection of mainly muscular arteries that begin at the sinus of Valsalva, where the ascending aorta gives rise to the right and left coronary arteries (RCA and LCA, respectively) from its right and left sinus openings.[29] The RCA and LCA will give rise to branches that will supply the entire myocardium. The LCA arises from the left aortic sinus and gives rise to the left circumflex artery and the anterior interventricular artery (left anterior descending; LAD). The RCA arises from the right aortic sinus and progresses laterally along the right side of the heart to give rise to vessels that mainly supply the right ventricle. In 90% of individuals, the RCA gives rise to the posterior interventricular artery: termed a right-dominated coronary circulation. Using arteriograms, Dodge *et al*.[30] indicated that normal vessel diameters of the LCA, proximal LAD, and distal LAD are 4.5±0.5 mm, 3.7±0.4 mm, and 1.9±0.4 mm, respectively with similar values obtained for the RCA and derivatives. The relative sizes between the sexes appear to vary significantly as documented in numerous studies.[31, 32] That said, the main deviation between individuals is the alteration in the mechanical properties of the coronary circulation with age. Specifically, the elastin-collagen ratio decreases with age from 5.43 to 2.57 in the LCA and 3.80 to 1.72 in the RCA.[31] The decrease in the ratio suggests the progression of stiffer arteries with age. However, ignoring the extremes of age, the typical mechanical profile of the coronary circulation is as follows: a burst pressure of 2000 mmHg

[33], a maximal circumferential strain reached at 20% distension[34], and a normal pressure exposure between 50-130 mmHg.[35]

2.3 Coronary Artery Disease (CAD)

Cardiovascular disease (CVD) represents the leading cause of mortality globally from which coronary artery disease (CAD) is the leading factor.[1, 36] The alarming trend is that the incidence and prevalence of CVD is increasing. In the United States, it is projected that approximately 40.5% of the population will be burdened with CVD and the associated costs are expected to exceed $800 billion by 2030.[37] With advances in healthcare, the morbidity of the disease and its complications are likely to parallel this trend in augmented prevalence as individuals live longer lives.

The main instigating factor in the development of CAD is atherosclerosis, a progressive disease characterized by gradual lumenal narrowing of blood vessels leading to compromised distal blood flow and tissue perfusion which results in potential ischemic complications.[38] The pathology increases in prevalence with age due to the progressive nature of the disease and repeated exposure to mostly modifiable risk factors. A main risk factor are increased levels of cholesterol and low-density lipoprotein (LDL), whereby the LDL functions to bring cholesterol and phospholipids to the peripheral cells and tissues rather than back to the liver for recycling as high-density lipoprotein facilitates.[39] Normally, LDL circulates within the plasma at low concentrations yet can be elevated due to a poor diet and diabetes, among other factors.[38, 40] If the endothelium is damaged, which is likely with hypertension and smoking, then LDL can accumulate within the sub-

endothelial space within the tunica intima. The resultant response, and the basis of the pathogenesis of atherosclerosis, is the "response to injury" phenomenon which is an immune mediated reaction to cope with the lipid insult and endothelial damage.[41] Resident tissue macrophages within the sub-endothelial layer attempt to phagocytose and remove the LDL. However, numerous free radicals and potential apoptotic debris are produced which facilitate the oxidation of LDL within the layer.[38] As the macrophages repetitively ingest the oxidized LDL, they transition in morphology to become foam cells. The pathology and lumenal narrowing becomes exacerbated by endothelial damage and the ability of oxidized LDL to act as a pro-inflammatory and adhesive mediator to circulating monocytes.[38]

The tunica intima has additional functions pertaining to anti-thrombotic activities under normal homeostatic conditions. The ECs are able to secrete numerous factors such as nitric oxide (NO) and prostacyclin (PGI_2) which attempt to mitigate adhesion and promote vasodilation. The initial sign of endothelial damage is a decrease in the levels of NO produced which consequently leads to lumenal narrowing which facilitates a greater concentration of circulating clotting and inflammatory factors that can interact with the endothelium.[42] It is the integrity of the endothelial lining that is paramount as the sub-endothelial matrix is highly thrombogenic *in vivo* with collagen and von Willebrand factor being able to interact with platelets. The damaged endothelium promotes the expression of specific adhesion molecules that are able to attract leukocytes to the area of damage such as P-selectin. An inflammatory cascade ensues whereby a fibrous plaque develops that attempts to cover the area of endothelial damage yet it will encroach and challenge the

integrity of the arterial lumen.[38] The response impacts the medial SMCs and the organization of elastin and other ECM proteins as SMC proliferation and protein production is stimulated. The resultant disorganization of the fibers further augments the stiffness of the blood vessel.[43] New tropoelastin may be secreted, yet it will not possess the same arrangement and thus the mechanical properties of the arteries will be significantly altered, especially as increased collagen is deposited due to the inflammatory process.

The patency of the coronary arterial circulation is essential to ensure sufficient perfusion to the myocardium. Coronary artery occlusion follows a gradual course initially characterized by stable angina which leads to unstable angina and ultimately the potential for myocardial infarctions. The classification of the varying states is based on the degree of vessel occlusion. Rarely, blockages occur as a result of an embolus and are usually associated with atherosclerotic plaques. With higher occlusion percentages, individuals begin to complain of exertional dyspnea as the decrease in lumenal diameter compromises myocardial perfusion resulting in the lack of sufficient oxygenation.[44] With progressive occlusion, a myocardial infarction may occur which is characterized by a massive compromise in cardiac output and potential conduction disarray which leads to death.

2.4 Therapeutic Interventions for CAD

The initial therapeutic approach should be centered on prophylaxis through lifestyle modifications and pharmacological therapy. The treatment is based on attempting to reduce myocardial oxygen demand, which beta-antagonists can provide, or to increase the caliber

of the coronary vessels and improve exercise tolerance, which is the indication for nitro-dilators. Additionally, aspirin or clopidogrel may be recommended to ease the concern of potential thrombi causing distal ischemia and complications. Unfortunately, the efficacy of lifestyle modifications and pharmacological therapy suffers from poor patient compliance.[2] More invasive interventions may be required if these techniques fail.

In the non-surgical setting, the approach is centered on revascularization of occluded coronary vessels and can be accomplished most commonly with percutaneous coronary interventions (PCI) which include balloon angioplasty and coronary stenting. PCI entails the insertion of a wire or catheter, usually into the radial artery, that is guided *via* imaging to the site of the coronary occlusion.[45] A meta-analysis comparing the efficacy of PCI versus conservative pharmacological therapy in chronic stable CAD indicated that PCI fails to offer any benefit in the management of these patients and may have additional risks.[46] The main concerns with PCI are the potential for stent restenosis due to increased disorganized cellular proliferation within and around the stent and the development of thrombus formation. It has been shown that the main response to the procedure is a significant increase in intimal thickening.[47] Balloon angioplasty has been shown to have a 30-60% risk of re-occlusion of the vessel whereas bare metal-stents have an approximate 16-44% risk in the development of restenosis.[48] To reconcile these risks, drug-eluting stents were developed, however complications can still occur in 3-20% of patients due to allergic reactions, granulomatous inflammation, and neo-intimal thickening.[49] With the development of more unstable ischemic inducing states, surgical interventions are considered as more potent re-vascularization strategies.

The standard surgical intervention is the coronary artery bypass graft (CABG). The procedure is based on transferring another vessel to replace the diseased artery. Most commonly, autografts are used such the great saphenous vein (GSV) or internal thoracic artery. However, a common occurrence is the presence of co-morbidities that make these vessels unusable or previous harvests have already removed them. Specifically, the GSV is usually found to be pathological when harvested, which emphasizes the need for consideration of other allogenic sources.[50] It is possible to harvest vessels from other donors or animals, yet significant immune-mediated issues arise due to their inherent thrombogenicity which has been shown to decrease the patency of the graft within a short time-frame post-operative in many patients.[51] Unfortunately, those with CAD are likely to have multi-vessel involvement. A recent meta-analysis comparing PCI to CABG for those with multi-vessel disease indicated that while CABG resulted in a slightly higher incidence of strokes, they did reduce the need for future re-vascularization and decreased long-term mortality.[52] A possible reason for the long-term advantageous use of CABG is that it may provide a more natural and tailorable environment for the cells to interact with. However, for small diameter graft replacements, no ideal solution exists as of yet and synthetic grafts produced *in vitro* are attempting to address this urgent clinical need.

2.5 Vascular Tissue Engineering (VTE)

2.5.1 Overview

Vascular tissue engineering (VTE) attempts to mimic the native vessel architecture and fabricate a mechanical analogue of the vessels that will be conducive to cell viability and

growth potential while maintaining long-term lumenal patency. In blood vessel tissue engineering, the goal is to fabricate a tissue that is mechanically competent and biologically responsive in a process that is highly reproducible and consistent. The creation of such an analogue is termed a tissue engineered blood vessel (TEBV). The classical paradigm of VTE involves the growth of cells in two-dimensional (2-D) culture and subsequent seeding onto a three-dimensional (3-D) substrate for maturation. Ideally, maturation will occur in a bioreactor to mimic the native hemodynamic forces the cells are exposed to *in vivo*. The VTE process description for the fabrication of a TEBV is outlined in Figure 2.4.

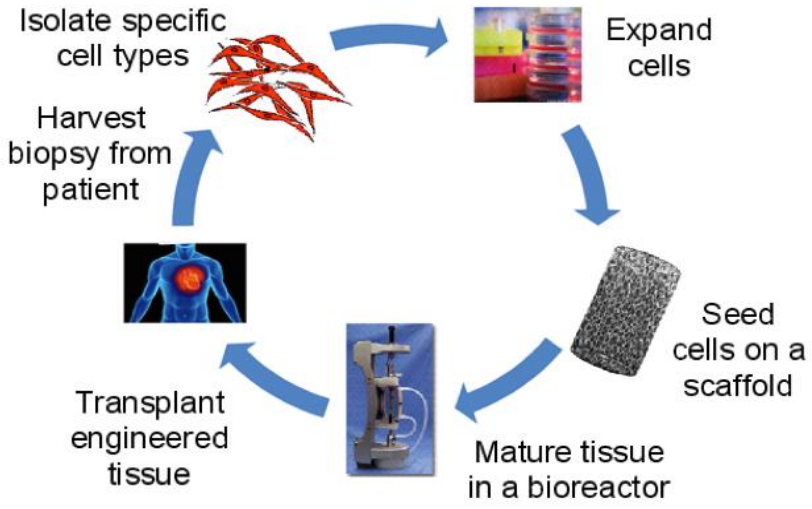

Figure 2.4: Process description for vascular tissue engineering (VTE). The overall approach is to harvest cells from patients, expand them in culture and seed them to a 3-D scaffold for maturation and remodeling in a bioreactor.

2.5.2 Cell Source

The cells utilized for VTE should reflect those found in native vessels, being some combination of fibroblasts, SMCs, and ECs that populate the three component vessel layers. ECs provide potent signaling to the underlying SMCs within the vessel which can direct ECM production and angiogenesis; the latter being highly important given the mass

transfer limitations of oxygen when vessel wall thickness is increased.[53] An intact endothelium significantly reduces the thrombogenicity of the graft at the early implantation stages – especially if seeded initially with venous ECs which have been shown to be less thrombogenic than arterial cells.[54, 55] Additionally, EC capture and seeding can be enhanced through the utilization of peripheral whole blood (PWB) as it contains numerous endothelial precursor cells that possess the capacity to differentiate into ECs if the correct milieu is provided.[56] For instance, the presence of a monolayer lining of ECs was observed when PWB was added to a decellularized allogenic scaffold.[57] Interestingly, when a graft is implanted into a patient, ECs have been shown to re-populate the lumenal lining *in vivo* with staining confirming the original seeded cells were replaced by native cells within an acute time-frame.[58] This suggests that vascular grafts may not necessarily need ECs when implanted given the ability of the ECs to re-populate the graft *in vivo*. However, if this were to occur, anti-platelet and anti-coagulative therapy should be provided until endothelialization occurs for the patient to be at low risk of developing thrombosis.[59]

Given the ability of ECs to re-populate the graft *in vivo*, the main challenge is how to best re-populate the graft with the cells that comprise the tunica media and adventitia.[60] Stem cells have emerged as a viable option as a cell source due to their potential to differentiate into SMCs. Bone-marrow mesenchymal stem cells, adipose derived stem cells, and human umbilical cord derived stem cells have shown the ability to express vascular SMC (vSMC) protein markers *in vitro* and mimic SMC-like ECM production.[61, 62] Specifically, mesenchymal stem cells are a preferred choice due to their ability to be expanded in culture and avoid immune-mediated responses while maintaining multi-potency and easy access

for harvesting.[63] While promising, studies are mixed in regards to the adverse effects *in vivo* with the use of mesenchymal stem cells which may limit their use until safety can be ensured.[64] Additionally, while stem cells can be coaxed into differentiating down a vSMC pathway, given the complexity of the process, a reasonable concern is the extent of the differentiation.[65]

As the differentiation process has not been optimized *in vitro*, the simplest way to ease this concern would be to utilize primary SMCs and fibroblasts - especially when attempting to investigate signaling pathways within grafts. However, primary SMC lines have been shown to have variable responses in culture that relate to the donor source.[66] SMCs sourced from older donors produce less collagen and elastin and have less proliferative capacity than their juvenile counterparts.[66, 67] Regardless of age, primary SMCs show a limited capacity for proliferation *in vitro*, where typically 10-30 population doublings occur prior to senescenece.[67] While stem cells are more robust, there exists ways to circumvent the growth retardation of vSMCs seen in 2-D culture. As an example, McFetridge *et al*. [68] demonstrated that bioreactor systems can induce SMCs to maintain their *in vivo* phenotypes. It is also possible that the utilization of higher initial seeding densities can circumvent the need for numerous population doublings to increase ECM production.

2.5.3 Scaffolds

The ideal scaffold is expected to mimic the geometry of the tissue to be fabricated and provide correct clues to the cells that are conducive to growth and ECM production. The scaffold should initially allow for suitable attachment and anchorage of the cells followed

by proliferation without a cytotoxic or inhibitory effect. The ideal scaffold candidate would therefore be native ECM itself, and this can be made possible through the use of decellularized scaffolds. The native ECM provides a rich source of proteins such as fibronectin that cells can interact favorably with the matrix.[69] However, decellularization procedures usually requires the use of detergents and proteases that may disrupt the normal architecture of the ECM and dislodge potential signaling and attachment components.[70] The decellularization procedure generally produces variable mechanical change in the scaffold, usually generating weaker grafts.[70] Since collagen and elastin are essential for the mechanical properties of arteries, their use has been investigated as a comparable option to that of decellularized scaffolds. However, it has been found that collagen itself may be a poor scaffolding material as it loses mechanical strength and stability upon hydration in addition to potential immune-mediated reactions and disease-risk when extracted from animal sources.[71] Recombinant technology is attempting to produce collagen, yet the process remains to be optimized and is not currently a viable option for VTE use.[70] A major issue with elastin-based scaffolds are their propensity to calcify *in vivo* which would mitigate the suitability of the scaffold as the mechanical properties are altered.[72] Another approach, which would allow more consistent optimization of the required mechanical properties, is the development of synthetic scaffolds. These scaffolds, if fine-tuned to match the required properties of the ECM, possess high viability to be mass-produced and available as an "off-the-shelf" option for surgical interventions.[73] Viable synthetic scaffolds include biodegradable polymers, such as polyglycolic acid (PGA), polycaprolactone (PCL), and derivatives synthesized *via* copolymerization with polymers, such as poly (lactic-co-glycolic acid), that aim to optimize degradation kinetics of the graft

in vivo.[74] The goal is to match the degradation rate *in vivo* with suitable ECM production without jeopardizing the mechanical properties as this occurs.[70]

Equally important to the scaffold material is the fabrication method. Electrospinning has emerged as a promising option for VTE due its ability to facilitate the fabrication of nanofibrous matrices that mimic the topography of the ECM. The technique involves subjecting a polymer solution to a high voltage which is ejected through a capillary in a dynamic unstable manner at a controlled rate. Once ejected, the electrical force is greater than surface tension which creates nanofibrous polymer mats.[75] The solvent is evaporated as random fibers are deposited onto a grounded collecting plate. However, while the fibers mimic the native ECM in morphology, it is difficult to control the exact orientation of the fibers and a major limitation with electrospinning is a lack of suitable cell infiltration due to small pore sizes.[76] Another technique that directly addresses this issue is utilizing hydrogels as the scaffolding material. Hydrogels are composed of hydrophilic polymer chains that are cross-linked allowing for the gel to swell when placed in an aqueous environment without a loss of structure.[77] The gel matrix allows for suitable mass transfer of nutrients and gases and additionally offers a way to ensure suitable cell encapsulation.[78] However, a major limitation with hydrogels is their lack of mechanical integrity, especially when utilizing natural polymers compared to synthetic options.[79] Another fabrication method is that of solvent casting and particulate leaching (SCPL). The technique involves dissolving a polymer in a suitable solvent and forcing the developing viscous solution through a porogen bed to which the porogen is leached out in a solvent that does not dissolve the polymer. The resulting construct will have a porous structure with high overall

porosity at the macro and micro porous levels. However, SCPL offers limited control over the orientation of the pores and the overall pore interconnectivity.[80] That said, the benefit of SCPL is that there is a high control over overall porosity and thus cell infiltration. Overall, SCPL offers a simple fabrication process with high tunability in a fabrication method that is cost-effective.[81]

2.5.4 Bioreactors

The use of bioreactors allows for simulation of the native hemodynamic forces. Forces such as shear stress on the ECs and the pulsatile nature of the blood flow can induce signaling events. Specifically, these forces have been shown to induce growth and maturation of the cells significantly different than that of static culture.[82] The stimulation induces the SMCs to secrete more ECM proteins and has been associated with improved graft mechanical properties.[83] Mechanical stimulation additionally allows vSMCs to adopt phenotypes more akin to the *in vivo* environment which may further explain the reasoning to these grafts developing higher mechanical properties and improved patency when cultured within a bioreactor.[84, 85]

2.6 Small-Diameter VTE: Challenges and Potential Solutions

Synthetic grafts made from expanded polytetrafluoroethylene (ePTFE) and polyethylene terephthalate (PET, Dacron™) work well for large diameter vascular graft replacements (>6 mm diameter) where the blood flow rate is high but results in small diameter coronary artery graft applications (<4 mm diameter) have been disappointing.[86-88] The main limitation with small diameter grafts is thrombosis which occludes the lumen and

exacerbates the pathologies the graft attempts to alleviate. A non-autologous vascular replacement will induce an immune response, yet the reaction may not necessarily be acute. Furthermore, if the mechanical properties of the graft are not matched with that of the native vasculature at the anastomotic sites, the generated turbulent flow induces an immune-mediated response that can result in lumenal occlusion.[89] These limitations prompted the field of VTE. Despite rapid advances made in this field, success has been limited due to significant knowledge gaps in our ability to control and coordinate cell phenotype and direct tissue formation, which is the ultimate goal for VTE.[90] Particularly, stimulating and understanding elastogenesis in VTE has been proven to be difficult.[3, 11, 91] It is understood that for a TEBV to be successful, it must incorporate elastin into the developing tissue construct to achieve the required overall viscoelasticity of the final tissue.[11, 92] It is possible that utilizing elastomeric scaffolds could be helpful for improving the elasticity of the engineered tissue. Indeed, the use of elastomeric scaffolds has resulted in more akin mechanical properties to that of the native arteries.[93, 94] There is optimism that a cell-free tissue engineering approach can be based on the use of such scaffolds.[95] Unfortunately, the approach relies on *in vivo* re-modeling and it can be expected that the results will be variable. Additionally, this technique relies on infiltration of native cells and an immune response to acquire the required remodeling. Yet again, this may vary from host to host and might not be suitable for the small diameter vasculature.[96] As such, while the synthesis of elastomeric scaffolds improves the mechanical properties, there is a need to seed cells prior to implantation. Ideally primary human coronary SMCs (hcSMCs) that are responsible for producing elastin and assembling it to elastic fibers within the medial layer would be utilized. If elastin can be produced at high levels and assembled into fibers,

then the mechanical properties of TEBVs can be expected to increase. An avenue that can be taken is the use of factors that can stimulate elastogenesis. However, in addition to their impact on elastogenesis, these factors may influence the phenotype of the vSMCs.

2.7 Vascular Smooth Muscle Cell (vSMC) Culture

2.7.1 vSMC Phenotype

vSMCs represent a dynamic cell line in which their phenotype is not terminally differentiated and rather exists as a continuum of states between synthetic and contractile.[97] During development, vSMCs begin in a highly proliferative synthetic state where ECM protein production is high. A transition occurs that decreases ECM production and increases intercellular myofilaments, a switch that facilitates the required contractility within blood vessel walls.[98] Studies have indicated that the transition can be bi-directional.[99, 100] The phenotypic plasticity can vary along the arterial tree during normal homeostatic conditions due to the presence of alternative populations of vSMCs.[101] However, *in vivo*, the phenotypic plasticity is correlated with pathological events such as seen in atherosclerosis whereby the usual contractile vSMCs in the medial layer can migrate to the intima and become synthetic, promoting intimal thickening and hyperplasia – an undesirable outcome. The continuum between synthetic and contractile is classically characterized by the presence or absence of specific proteins.[97] The contractile state contains minimal rough endoplasmic reticulum and ribosomes indicating that its function is not related to extensive ECM protein synthesis.[101] When the vSMCs are in the contractile state, they have a large volume fraction of myofilaments within their cytoplasm.[98] The contractile proteome of these cells indicate high expression of

contractile protein markers such as smooth muscle alpha actin (α-SMA), calponin, SM-22α, and smoothelin.[101] De-differentiation into the synthetic phenotype is associated with a loss of these markers.[101] In addition to quantitative changes in the contractile protein markers, the modulation in phenotype is also associated with alternative rearrangements and realignments of the myofilaments.[102] Due to the lower level of protein secretion, the contractile vSMCs are denser and more fusiform in nature, a stark contrast to the expansive, broad, and fibroblast-like epithelioid morphology of the synthetic phenotype. When cells de-differentiate into a synthetic phenotype, a loss of the high volume of myofilaments, a disappearance (or reduction) of the contractile markers, and an increase in apparatuses promoting protein production have been observed. Specifically, elastin production is likely correlated with the synthetic vSMCs phenotype, yet there has been mixed results.[103, 104] In contrast to the contractile upregulation of vSMC protein specific markers, it is thought that the synthetic phenotype is characterized by a disappearance of the contractile markers. However, proteins such as L-caldesmon and meta-vinculin can be used to denote the synthetic state, yet marker specificity for the synthetic phenotype is not as specific as the contractile state.[105]

2.7.2 vSMC Response to Microenvironments: 2-D vs. 3-D Culture

Classically, most cell culture investigations have been performed on a 2-D surface yet this is an inaccurate representation of the *in vivo* environment. While 2-D culture is a quick and well-established culture system, it only provides a simplistic and limited substrate that cells can interact with. Within the ECM, cells are constantly exposed to varying topologies, gradients, and forces – all of which are difficult, if not impossible, to replicate in a 2-D

setting. It can be expected that cells will respond and behave differently when seeded in 2-D and 3-D environments. When cultured in 2-D, most vSMCs are known to adopt a more synthetic phenotype compared to a contractile state usually seen *in vivo*.[101, 106] Yet, most early experimental designs considered vSMCs only in a 2-D environment, one that is stiffer than the native ECM found in blood vessels. Indeed, a major difference between 2-D and 3-D is the stiffness of the underlying substrate. Recently, Timraz *et al.* [107] demonstrated that collagen-I gels with varying degrees of stiffness can influence vSMC phenotypic differentiation and protein secretion with the synthetic phenotype being inversely proportional to increasing the stiffness of the gels. However, the study investigated cellular responses when encapsulated in a collagen gel and when combined with various ECM proteins, such as fibronectin, which may influence the manner in which the cells interact and spread within the matrix as the supplemented factor concentration is increased. The exact experimental design for investigating how cells respond to variant stiffness in 3-D remains to be optimized. This may be due to designs that increase the cross-linking density, consequently increasing the propensity for cell-mediated proteolysis and subsequent migration.[108] A commonality between how the cells sense stiffness in 2-D and 3-D is through RhoA, a small GTPase that facilitates mechanotransduction. RhoA activation has been shown to be upregulated in 2-D culture and in atherosclerosis.[109] When RhoA is constitutively expressed in vSMCs in 3-D cultures, the state of vSMC differentiation has been shown to depend on the stiffness of the substrate and produced similar cytoskeletal effects seen in 2-D culture.[106] Upregulation of RhoA in vSMCs is associated with ***an*** increase in contractile SMC markers in 3-D.[106] While stiffness may have an effect on the phenotype, the 3-D environment additionally changes the mechanism in which the cells are

able to sense their surroundings. Using varying matrices, Hong *et al*.[110] demonstrated varying temporal differences in ECM expression in 3-D relative to 2-D with significant variability when alternative 3-D scaffolds were used. Work by Lin *et al*. [111] also demonstrated that hcSMCs seeded in 3-D expressed higher levels of elastin than in 2-D culture. However, when TGF-β1 was utilized to increase elastin, the up-regulated elastogenic effect was noticed only in 3-D and not in 2-D suggesting that the effect of TGF-β1 in 2-D cultures may not translate to 3-D. Another biochemical factor that is elastogenic but not widely studied is retinoic acid which is a vitamin A derivative. Since this thesis focuses on retinoic acid, an expanded review is presented in the proceeding section.

2.8 Retinoids

2.8.1 Overview

Retinoids are derivatives of vitamin A that are highly active during embryogenic development and have been shown to have a positive impact on elastogenesis. Four of the biologically active derivatives are retinol, retinal, 9-cis retinoic acid (9cRA), and all-*trans* retinoic acid (atRA).[112] While there are numerous metabolites, it is atRA which is the carboxylic acid form that has been shown to have the most potent biological activity.[113] It should be noted that there have been reports indicating isomerization potential between atRA and 9cRA intracellularly.[113] As a lipophilic molecule, the atRA concentrations within the plasma are low - ranging between 1-10 nmol/L.[113] Most *in vitro* experiments with atRA utilize the relevant therapeutic and physiological concentration, corresponding approximately to 1 μmol/L.[113] Due to its lipophilicity, a retinol binding protein (RBP) associates with atRA within the plasma and carries the molecule to target organs.[114] The

atRA is able to diffuse past the cellular membrane and an interaction can occur with a cellular retinoic acid binding protein (CRABP). There are two isoforms of CRABP, being I/II, though only CRABP-I has been shown to be relevant in vSMCs.[115] Binding to the CRABPs occur with high affinity and seems to increase the ability of atRA to be translocated to the nucleus.[116] Within the nucleus, the complex interacts with two subsets of nuclear receptors being the retinoic acid receptor (RAR) and retinoid X receptor (RXR)[113], to which there are 3 isoforms of each (α, β, and γ).[117, 118] Both receptors associate as a heterodimer that are bound to a retinoic acid response element (RARE) near specific target genes that normally act to repress transcription. Retinoids are able to bind to the RAR allowing for conformational changes to be induced that create positive transcriptional effects. Both 9cRA and atRA are able to bind to the RAR yet only 9cRA can associate directly with the RXR. However, the RXR itself has not been proven to have physiological relevance. An overview of the metabolism and subsequent processing of atRA is shown in Figure 2.5.

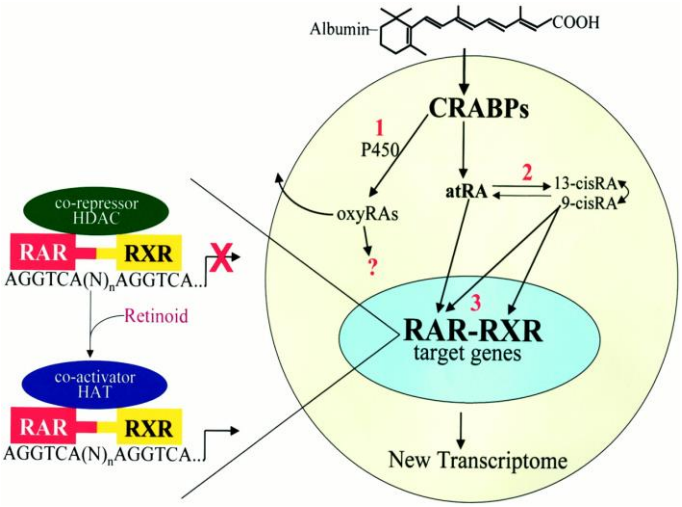

Figure 2.5: Intracellular effects of atRA. After being transported through the plasma by a protein carrier, albumin, atRA translocates across the membrane and associates with the CRABPs that allow nuclear translocation and subsequent transcriptional effects.[113] Used with permission from the Publisher.

2.8.2 atRA Impact on vSMC Phenotype

The current understanding of the effect of atRA on vSMC phenotype is that an anti-proliferative and differentiated state is induced. Interestingly, atRA is being investigated for its role is preventing intimal thickening and restenosis following PCI.[4] The elevated levels of contractile makers have been associated with atRA possessing potential negative effects on growth and cellular proliferation in human tissue culture. Axel *et al*.[119] found that in a dose-dependent manner, atRA decreases both proliferation and migration. The ability to produce the latter effects may be attributed to a retinoid-inducible tissue trans-glutaminase (ttG).[120] Recently, *in vivo* experiments confirm that atRA can inhibit vSMC proliferation and promote contractile marker expression *via* upregulation of Kruppel-like Factor 4 (KLF4), a zinc-finger transcription factor.[121] KLF4 activation has been shown to activate p53 to inhibit vSMC proliferation.[122] Knockdown studies of KLF4 mitigated the atRA mediated increase in contractile protein markers being α-SMA and SM-22α.[123] In rat vSMCs, atRA has been shown to increase the levels of contractile markers such as α-SMA.[124] The increase in these markers was associated with a stimulation in protein kinase C-α activity.[124] However, it is not intracellular interference alone that atRA exerts its anti-proliferative effect, as it has been shown to influence ECM production. Perlecan sulfate is a large proteoglycan within the ECM that has been shown to have anti-proliferative properties. When transgenic mice were engineered to be deficient in perlecan sulfate expression, the atRA mediated anti-proliferative effect was depressed.[125] That said, most of the above studies occurred in 2-D culture. The phenotype adopted by vSMCs in response to atRA treatment may be dependent on the initial state of the cells.[126] The

different responses obtained in early investigations may be due to the source of vSMCs and the experimental design.

2.8.3 atRA Impact on Elastin Expression

The effects of atRA seems to be tissue-dependent with pleiotropic impact.[113] In terms of elastogenesis, atRA has been shown to have potent impact on the pulmonary and arterial circulations and is associated with dermal elasticity.[127-129] The earliest studies suggesting atRA may increase elastin occurred in pulmonary lung fibroblasts based on observations that elastogenesis within the alveolar septa correlated with atRA levels during brief periods in postnatal life.[130] For the pulmonary circulation, elastin is essential for lung compliance and proper breathing mechanics. Indeed, deletions in RARs, specifically RARγ, have corresponded to reduced elastin and alveolar numbers.[131] Similar pathological manifestations occur within the vasculature when atRA signaling pathways are interfered with. Pathologies that result from low retinoid levels include an increased mortality from CAD.[132] Within the arterial tree, the derivatives of vitamin A with the greatest elastogenic impact are 9cRA and atRA.[133] In aortic SMCs harvested from 18-day old chick embryos and cultured on 2-D surfaces supplemented with atRA, elastin synthesis increased in a dose-dependent manner while cell number was decreased compared to the control.[133] This suggests that if atRA is to be used in VTE, higher cellular seeding densities should be utilized.

2.8.4 atRA in Combination with Ascorbic Acid: Impact on Elastin

Ascorbic Acid (AA) is added to cell culture experiments due to its potent effect on collagen synthesis in numerous cell types.[134-136] However, supplementation with AA in 2-D culture attenuates elastogenesis in a concentration dependent manner. AA can influence elastogenesis at both the transcriptional and post-transcriptional stages by reducing total transcript number and tropoelastin mRNA stability.[137] There may be an interplay between the two factors on elastogenesis in long-term cultures. While AA can increase the mechanical properties of the engineered tissue, the resulting increase in stiffness due to a lack of elastogenic stimulation may result in a vessel that does not mimic the *in vivo* scenario.[138] While atRA was added to mitigate the loss of elasticity, the combination of both seemed to have a complex impact on elastogenesis.

2.9 Study Rationale and Objectives

Within the VTE field, a major limitation is the inability to properly recapitulate the mechanical properties of a native tissue. Specifically, *in vitro* elastogenesis has proven to be difficult while collagen production can be sufficiently stimulated. It is necessary to increase both collagen and elastin synthesis to ensure the engineered vessel has suitable mechanical properties. As the goal would be to increase elastin expression, biochemical factors can aid in stimulating elastogenesis. Specifically, we suspect that atRA can increase elastin expression in 3-D cultures. However, as there is a need to promote collagen synthesis too, AA and atRA may have significant effects on the phenotype of vSMCs that could be relevant to elastogenesis. In doing so, better understanding of the interaction

between AA and atRA may lead to the engineering of functional vascular substitutes. In view of the above, the objectives of this study were to:

i) Fabricate and characterize PCL scaffolds with suitable porosity conducive to cellular infiltration and proliferation and

ii) Evaluate elastogenesis when hcSMCs are seeded on PCL scaffolds and treated with AA and atRA individually or in combination

Chapter 3 – Materials and Methods

3.1 Materials

ε-Polycaprolactone (PCL; M_n=80,000 Da) was used to fabricate the 3-D scaffolds and was obtained from Sigma Aldrich (Oakville, ON, Canada). All solvents used to dissolve the PCL pellets were obtained from Caledon Labs (Georgetown, ON, Canada) and included chloroform ($CHCl_3$), ethyl acetate (EtOAc), and tetrahydrofuran (THF). Ammonium chloride (NH_4Cl) was supplied by Caledon Labs and was utilized as the porogen for the 3-D scaffolds. Cell culture experiments were conducted on primary hcSMCs in Medium 231 supplied by Life Technologies (Burlington, ON, Canada) and on immortalized NIH-3T3 fibroblasts in DMEM obtained from Lonza Walkersville Inc. (Walkersville, MD, USA). Medium 231 was supplemented with 5% penicillin G and streptomycin sulfate (P/S), insulin-like growth factor (IGF), and basic fibroblast growth factor (bFGF). DMEM was supplemented with 10% fetal bovine serum (FBS) and 5% P/S. All components added were obtained from Life Technologies. Cellular washing steps were conducted in Hank's Balanced Salt Solution (HBSS) supplied by Life Technologies. L-ascorbic acid (AA) and all-*trans* retinoic acid (atRA) were obtained from Sigma Aldrich. For cell fixation and immuno-histochemistry, a 4% paraformaldehyde solution in diH_2O was prepared from paraformaldehyde obtained from EMD Chemicals (Gibbstown, NJ, USA). Immunostaining utilized Alexa Fluor® 488 Phalloidin and DAPI (4',6-diamidino-2-phenylindole) supplied by Life Technologies. Mounting medium was obtained from Vector Laboratories (Burlington, ON, Canada). For qPCR, initial RNA isolation occurred utilizing Trizol® Reagent supplied by Life Technologies. Glycogen and iQ™ SYBR®

Green Supermix, used in the RNA purification and cDNA synthesis respectively, were obtained from Bio-Rad (Mississauga, ON, Canada). RNA work utilized a NanoDrop Lite Spectrophotometer obtained from Thermo Scientific and a C1000 Touch™ thermal cycler (CFX96™ Real-time system) supplied by Bio-Rad. Protein quantification for western blotting was based on the construction of a standard curve utilizing bovine serum albumin (BSA) supplied by Sigma Aldrich. Protein quantification was completed using the 660 nm protein assay supplied by Thermo Scientific (Ottawa, ON, Canada). For western blotting, monoclonal (α-SMA and GAPDH) primary antibodies were obtained from Santa Cruz Biotechnology (Dallas, TX, USA) and EMD Millipore (Temecula, CA, USA) respectively. Polyclonal primary antibody against elastin was supplied by EPC (Owens, MO, USA). Secondary anti-rabbit and anti-goat HRP-conjugated antibodies were supplied by Santa Cruz Biotechnology. SuperSignal® West Pico Chemiluminescent Substrate was supplied by Thermo Scientific (Rockford, IL, USA). ChemiDoc™ XRS$^+$ and ImageLab™ software, obtained from Bio-Rad, were utilized to image and quantify the membranes respectively.

3.2 Methods

3.2.1 Scaffold Fabrication *via* Solvent Casting and Particulate Leaching (SCPL)

Tubular PCL scaffolds were fabricated using a solvent casting and particulate leaching (SCPL) method based on previous established protocols in our laboratory.[139] Briefly, NH_4Cl particles were mechanically processed using a mortar and pestle prior to passing through graded sieves to obtain porogen particle sizes between 180-210 μm. The collected particles on the 180 μm sieve were re-sieved once, to ensure they fell within the desired range. PCL pellets were dissolved in various solvents ($CHCl_3$, EtOAc, THF) at 40 °C and

varying concentrations, ranging from 10-30% w/w. To prepare the porogen bed, the NH_4Cl particles were packed into the annulus of a glass tube with a central mandrel. The polymer solutions were then infiltrated over the porogen bed using a pressure differential created by applying vacuum to the inferior aspect of the porogen bed. The glass rod was then removed from the apparatus and left upright in a fume hood for 2 hours prior to removal of the scaffolds from the glass rod. The scaffolds were kept for approximately 12 hours, to dry and allow for solvent evaporation, in the fume hood prior to placement into diH_2O. The tubular scaffolds were cut into small rings cut using a microtome. Rod-like porous scaffolds were also fabricated by removing the mandrel during the porogen packing. The SCPL apparatus is shown in Figure 3.1.

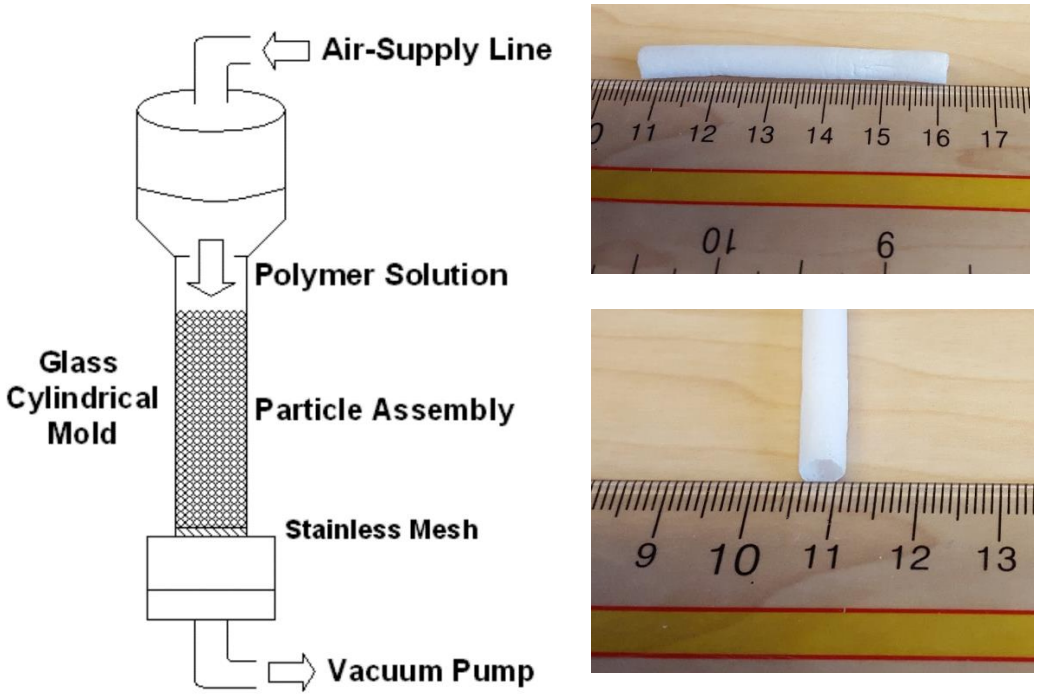

Figure 3.1: Solvent casting and particulate leaching apparatus. The digital images shown are the tubular scaffolds fabricated using the apparatus.

3.2.2 Scaffold Characterization

3.2.2.1 Scanning Electron Microscopy (SEM)

A scanning electron microscope (2-2600N, Hitachi, Japan) was utilized to assess the fabricated scaffold morphology. The scaffolds were sectioned into pieces of varying lengths to investigate the lumenal, ablumenal, and cross-sectional morphologies. The scaffolds were cut using a microtome and affixed *via* carbon tape to studs prior to gold sputtering and subsequent imaging.

3.2.2.2 Microcomputed Tomography (micro-CT)

Scaffolds were sectioned with a microtome into slices 4 mm in length. Imaging occurred using the eXplore Locus SP (GE Healthcare, Canada). Two different batches of scaffolds were scanned at a voxel resolution of 11 μm, using an integration time of 1700 ms per frame with 15 views per frame over 900 views encompassing 360^0. The x-ray tube voltage and current were set at 80 kVp and 90 μA respectively. The 2-D images obtained were compiled to generate 3-D representations of the scaffold architecture. A commercially available trabecular bone analysis software (MicroView version Viz+2.0, GE HealthCare) was utilized to analyze the 3-D images. Data analysis considered overall porosity, pore size, surface area to volume ratio, and strut thickness.

3.2.3 Cell Culture Conditions

Primary hcSMCs, between passage 4-8, were cultured in Medium 231 supplemented with bFGF, IGF, and 5% P/S. NIH-3T3 fibroblasts, between passages 6-15, were cultured in DMEM supplemented with 10% FBS and 5% P/S. Cell culture occurred within a 37 ^{0}C

sterile incubator at 5% CO_2. When factor addition was considered, all media changes occurred daily in the dark.

3.2.4 Scaffold Preparation for Cell Culture

Cylindrical scaffold sections, approximately 1 mm in length, were affixed with silicone grease. 10 scaffolds per 3.5 cm culture dish or 1 scaffold per 96-well plate were used. The scaffolds were immersed in EtOH overnight under UV light at RT in a sterile fume hood. The EtOH was aspirated and replaced with HBSS for pre-conditioning at 37 ^{0}C. Three aspirations of the HBSS were completed over the course of 12 hours to ensure removal of any residual EtOH.

3.2.5 2-D and 3-D Culture

Experiments in 2-D were carried out with hcSMCs seeded at densities of 250,000 cells/ 3.5 cm diameter dish. L-AA and/ or atRA addition occurred once the cells reached confluency and was termed day 0 in biochemical factor related experiments. Experiments in 3-D were carried out on hcSMCs and NIH-3T3 fibroblasts. The hcSMCs were seeded at a density of 450,000 cells/ scaffold. The NIH-3T3 fibroblasts were seeded at a density of 900,000 cells/ scaffold. Cells were allowed 24 hours for attachment prior to addition of L-AA and/ or atRA which was termed day 0 in biochemical factor experiments.

3.2.6 Cell Viability and Proliferation Assays

3.2.6.1 MTT

NIH-3T3 fibroblasts and hcSMCs were seeded onto 20%, 25%, and 30% PCL scaffolds prepared w/w in EtOAc. Cell culture occurred for 4 and 7 days at which time the media was aspirated and the cells were washed 1x gently in HBSS prior to the addition of 0.05% Trypsin-EDTA solution and incubation at 37 °C for 3 minutes. The solution was centrifuged and the pellet re-suspended in phenol red free medium. Addition of the MTT reagent, 3-(4,5-dimethylthiazol-2-yl)-2,5-diphenyltetrazolium bromide, was added to each well at a final concentration of 1.10 mM. The mixture was incubated at 37 °C for 1 hour proceeded by the addition of an equal volume of SDS (10% w/v in diH_2O) and the absorbance was read at 570 nm by a plate reader. The phenol red free medium was added to each plate as a blank.

3.2.6.2 DNA Quantification

The proliferative capacity of hcSMCs was investigated using the CyQUANT® cell proliferation assay, obtained from Thermo Scientific, and following the manufacture's protocol. Briefly, primary hcSMCs were seeded at a density of 500 cells/ scaffold in 96-well plates on 30% PCL scaffolds prepared w/w in EtOAc. After either 4 or 7 days, 0.05% Trypsin-EDTA solution was added and the scaffolds were incubated at 37 °C for 3 minutes. Scaffolds were centrifuged for 5 minutes at 4000 rpm and the supernatant removed prior to cellular pellet freezing at -80 °C. CyQUANT GR dye/ cell-lysis buffer was added to the pellets and fluorescence was read at 562 nm. A cell number standard curve allowed for quantification of growth over time.

3.2.7 Immunofluorescence Staining and Confocal Imaging in 3-D Culture

Cell cultures with primary hcSMCs on 3-D porous scaffolds were stained for F-actin and nuclei prior to imaging. Cells were fixed in 4% Paraformaldehyde for 1 hour at RT prior to cell permeabilization with 0.5% Triton X-100 for 10 minutes in 1x PBS. Following permeabilization, 2x washing steps for 5 minutes were completed in 1x PBS. Incubation for 1 hour at RT with diluted Alexa Fluor® 488 Phalloidin (1:50) in 1% BSA/PBS followed with 2x subsequent washing steps in 1x PBS for 5 minutes. Incubation with secondary antibody occurred for 1 hour at RT followed by 1x wash in 1x PBS for 5 minutes. DAPI staining was done for 10 minutes at RT prior to 1x wash in 1x PBS for 5 minutes. Scaffolds were affixed to glass microscope slides in mounting medium whereby spacers held the samples in place. A Zeiss LSM 510 confocal microscope (Carl Zeiss, Germany) was utilized in the imaging of the cells on the 3-D scaffolds.

3.2.8 RNA Isolation and Gene Expression Studies Using Real-Time PCR (qPCR) Analysis

Real-time polymerase chain reaction (qPCR) was used to quantify mRNA expression of GAPDH and elastin in primary hcSMCs seeded in 2-D culture. Total RNA was extracted *via* Trizol® Reagent to which 0.50 μg glycogen was added during the purification as described in the manufacture's protocol. The RNA pellet produced during the purification procedure was re-suspended in 20 μL dcpH_2O and quantified using a NanoDrop Lite Spectrophotometer. cDNA synthesis utilized 1 μg of total RNA, SsoAdvanced™ SYBR® Green Supermix, and 20 μM of GAPDH and elastin forward and reverse primers. The primers were as follows: GAPDH forward primer, 5'-GTT GGT CTC TGA CTT CAA

CA-3', and reverse primer, 5'-GTT GCT GTA GCC AAA TTC GTT GT-3'; elastin forward primer, 5'-AAC CAG CCT TGC CCG C-3', and reverse primer, 5'-CCC CAA GCT GCC TGG TG-3', were utilized.[140, 141] The qPCR protocol followed was specific for the SsoAdvanced™ SYBR® Green Supermix as per Bio-Rad. Samples were prepared in three replicates per experimental group and expression was normalized to GAPDH. Gene expression Macro Analysis Software was utilized for quantification.

3.2.9 Protein Analysis Using Western Blotting

A Lysis Buffer (LB) was prepared with final concentrations of 1x proteinase inhibitor cocktail, 1x PMSF, and 1x RIPA buffer all in diH_2O. For 2-D culture, plates were washed in 1x ice-cold PBS 3x prior to direct addition of LB to the culture plates followed by scrapping and freezing at -80 °C. For 3-D, the individual scaffolds were washed 3x in ice-cold 1x PBS prior to freezing at -80 °C. Once frozen, scaffold pieces were cut using a scalpel blade and added to LB and 3x freeze-thaw cycles occurred between -80 °C and RT. All subsequent work ensured protein samples were kept at least at 4 °C. Centrifuging occurred at 12,200 RPM at 4 °C for 12 minutes. The supernatant was collected and diluted 1:4 for protein quantification based on a BSA standard curve read at 562 nm. Resolving gels were prepared at 10% and stacking gels were prepared at 6%. Approximately 20-30 µg of total protein was loaded into the gels with each sample being composed of a final concentration of 1x Laemmli Sample Buffer with 1% beta-mercaptoethanol. Samples were heated at 95 °C for 5 minutes and briefly micro-centrifuged prior to loading. SDS-gels were run for 1 hour at 160 V. Transfer occurred for 1 hour at 90 V with numerous ice-packs to ensure the temperature was low on the nitrocellulose membranes submerged in a Tris-

glycine buffer containing 20% methanol. Ponceau S staining was subsequently utilized to qualitatively assess transfer efficiency. Blocking the membrane occurred over 1 hour in a solution containing 5% skim milk powder and 0.55% tween-20 in 1x PBS. Primary antibody incubation occurred overnight at 4 ºC in incubation buffer consisting of 0.1% skim milk powder and 0.11% tween-20 in 1x PBS. Primary antibody dilutions were made: α-SMA (1:500), GAPDH (1:1000), and elastin (1:250). After overnight incubation, 3x washing steps in incubation buffer occurred prior to incubation for 1 hour with HRP-conjugated secondary antibodies diluted (1:250) in incubation buffer. A further 3x washing steps in incubation buffer were completed prior to addition of the SuperSignal® West Pico Chemiluminescent Substrate. A ChemiDoc™ XRS system, from BioRad, was used to visualize the blots with further quantification occurring using ImageLab™ software.

3.2.10 Statistical Analysis

All protein quantification occurred using GraphPad Prism 5. Quantified data from qPCR and western blotting experiments was normalized to controls with no factor treatment in addition to GAPDH. Graphs were based on values obtained from three independent experiments. The data is displayed as mean ± standard deviation. The data was statistically analyzed by a one-way ANOVA proceeded by Tukey's post hoc test or an unpaired Student's *t*-test. *P*-values of <0.05 were considered to be statistically significant.

Chapter 4 – Results and Discussion

4.1 Scaffold Characterization

4.1.1 General Observations during Scaffold Fabrication

An ideal scaffold would be of comparable topography to that of the native ECM and possess suitable porosity internally with lumenal and ablumenal surfaces conducive for cell infiltration. An essential corollary to this notion is that the scaffold must possess the correct micro-structure to allow for the required cell attachment and proliferation.[142] Additionally, the scaffold should ideally be biodegradable with the degradation rate matching cellular ECM production to maintain mechanical integrity. PCL has been shown to meet the above requirements, with its *in vivo* degradation products being non-toxic while possessing the ability to be enzymatically and hydrolytically degraded.[143, 144] However, PCL degrades slowly (2-3 years) as the polymer is more so bioresorbable rather than biodegradable.[144, 145] This may be advantageous as it provides sufficient time for cells to regenerate their own ECM, if further *in vivo* remodeling is needed. That said, the optimal amount of time to match ECM production rates with biodegradation remains unknown.[146]

Previous investigations using PCL have been focused on electrospinning applications except a few studies which investigated PCL utilizing the SCPL process. Given the limitations of cell infiltration with electrospinning[76] and the potential for the seeded cells to therefore sense a more 2-D environment[147], it was thought that SCPL would be more appropriate – especially when investigating cellular activity differences to biochemical factors in 2-D compared to 3-D. Since PCL has not been extensively fabricated by SCPL,

there was a need to study this fabrication process. The variables considered in the SCPL process are outlined in Table 4.1.

Table 4.1: Variables considered for solvent casting particulate leaching (SCPL) process to fabricate PCL Scaffolds.

Variables	
PCL concentration (w/w)	10, 15, 20, 25, 30%
Solvent	$CHCl_3$, EtOAc, THF
Hold time in the tube (hours)	1, 2, 4, 6, 12, 24
Mandrel Materials	Teflon™ and stainless steel

Both tubular and rod-like scaffolds were fabricated. For the tubular scaffolds, a 4 mm mandrel was utilized and the resulting scaffold possessed an approximate 0.5 mm wall thickness to reflect the average size of a typical coronary vessel.[30] During scaffold fabrication, the scaffolds were kept upright in a glass rod for 2 hours before removing them from the mandrel and outer glass casing in order to evaporate part of the solvent and prevent scaffold damage. The 2 hour hold time in the glass rod was found to be optimal as longer times resulted in the scaffold hardening in the glass rod and thus was difficult to remove without damage. Scaffolds removed with hold times less than 2 hours were too weak and generally disintegrated upon removal. PCL concentrations greater than 30% were too viscous to be poured over the porogen bed and those less than 20% produced scaffolds with poor structural integrity and presented a challenge to consistently produce. Additionally, the fabrication of the cylindrical rod-like scaffolds were found to require longer wait times after removal from the scaffold fabrication chamber. This was likely due to the time needed

to evaporate the solvent and, perhaps, for the PCL to undergo some recrystallization which has been shown to generally result in an improvement of its mechanical properties.[148]

Regardless of initial PCL concentration for the rod-like cylindrical scaffolds, if these scaffolds were inserted into the deionized H_2O prematurely, the cross-sectional integrity was compromised and overnight incubation at RT was the optimal way to prevent this occurrence. An issue of structural/physical instability was observed in the rod-like cylindrical scaffolds at 10% and 15% concentrations whereby an unexpected hollow lumen-like structure was observed. This effect was seen with both hydrophobic ($CHCl_3$ and EtOAc) and hydrophilic solvent (THF) systems. Although a structurally stable PCL scaffold was not possible below a 20% concentration, Lin *et al*.[149] fabricated polyurethane scaffolds at 15% concentrations in dimethylformamide. It is likely that the molecular weight differences between these polymers represent one factor. The extensive hydrogen bonding that exist within polyurethanes is also a factor since solution viscosity increases with increased intermolecular forces.[150]

4.1.2 Scanning Electron Microscopy (SEM)

As the 2 hour hold time in the glass tube was optimal for the scaffold fabrication process, this time was chosen for subsequent scaffold fabrications. The SEM images for the tubular scaffolds are presented in Figures 4.1, 4.2. and 4.3. The ablumenal and lumenal surfaces were examined for their porous morphology. It was thought that the SCPL process would produce ablumenal and lumenal surfaces that were porous which would be beneficial for cell seeding, infiltration, and mass transfer.[151] Additionally, having a more porous lumenal

surface has been shown to make grafts less thrombogenic when implanted.[152] As the porogen was in close proximity to the glass rod or central mandrel, this was thought to facilitate an easier leaching out of the porogen and thus ensuring surface porosity. The effects of the organic solvent used to prepare the solution and the PCL concentration on the morphology of the tubular scaffolds is shown in Figures 4.1 and 4.2 respectively.

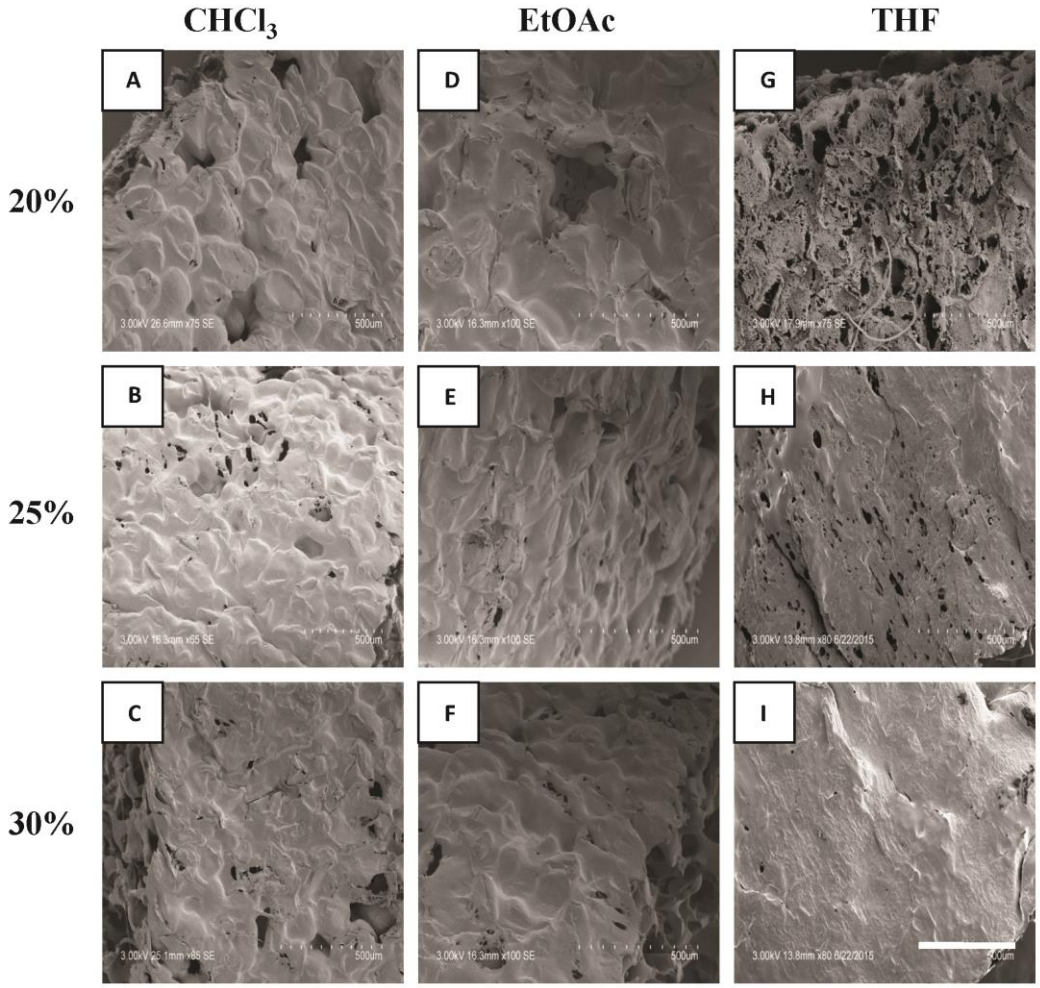

Figure 4.1: Ablumenal SEM images of 20-30% w/w PCL scaffolds fabricated using SCPL. PCL was dissolved in CHCl3 (A-C), EtOAc (D-F) and THF (G-I). Scale bar represents 500 μm.

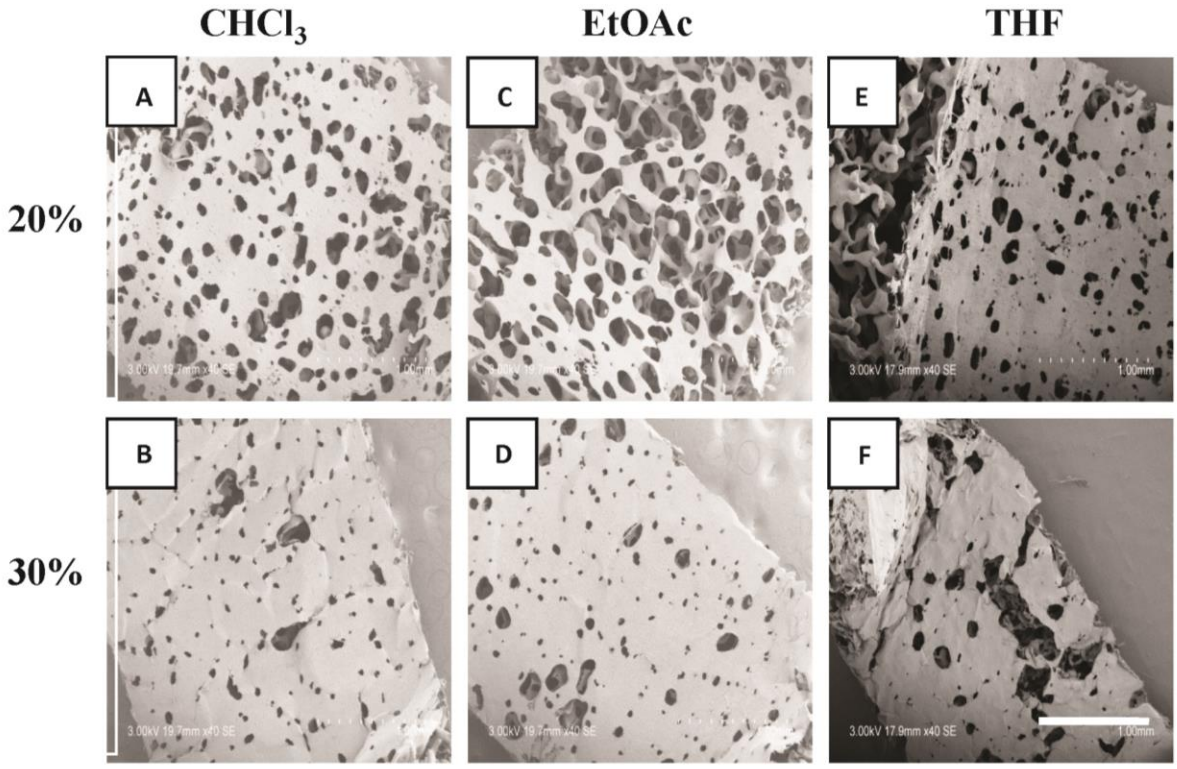

Figure 4.2: Lumenal SEM images of 20-30% w/w PCL scaffolds fabricated using SCPL. PCL dissolved in CHCl3 (A, B), EtOAc (C, D) and THF (E, F). Scale bar represents 1000 μm.

Regardless of solvent chosen and the PCL concentration, there appeared to be bubble-like films on the ablumenal surfaces. Since it was expected that the SCPL would produce scaffolds of varying porosity, the skin-like layer formation on the ablumenal surface was not anticipated. Interestingly for the lumenal porosity, the 20% concentration was better than the 30% concentration irrespective of the solvent used but these pores were isolated and not interconnected. The challenge is that both the ablumenal and lumenal surfaces did not produce consistently porous structures at all concentrations and instead morphologically resembled films. Despite using ammonium chloride porogens, the albumen and lumen morphologies observed in this study were consistent with a prior study that showed the solvent utilized to dissolve PCL dictated the surface morphology of casted

films due to the solubility of PCL in the various solvents with differences occurring at each interface, either glass or air.[153] In this cited study, film microporosity was observed at the polymer-glass interface when utilizing $CHCl_3$ and THF but not EtOAc. However, in the current study, all solvents appeared to produce similar effect on scaffold morphology when in contact with the steel mandrel in the lumen or the glass tube in the ablumen. The variation between the lumenal and the ablumenal surfaces likely reflect the different surface properties between the two materials. Although surface contamination was a possibility, both the glass rod and steel mandrel were washed in the respective solvent for each specific run and left to air dry prior to use – making this unlikely to be a confounding influence. To evaluate if the surface chemistry of the mandrel had any effect, a Teflon™ rod was utilized as a replacement for the steel mandrel on the basis of its low surface energy which may alter interface phenomena.[154] However, similar morphological effects were observed with the replacement mandrel (data not shown).

In addition to the lumen and albumen, the cross-section morphology was also investigated (Figure 4.3). With the exception of scaffolds fabricated using THF as a solvent (Fig. 4.1 F, H, I), all scaffolds were porous, interconnected, well-defined and open-faced. In the case of THF, however, the pores were not interconnected and the pore interconnecting windows were also sparse. A recent work by Choudhury *et al*.[155] suggested that the solvent may play a significant role in altering the porosity of PLA scaffolds fabricated using SCPL. The $CHCl_3$ and EtOAc however appeared to produce cross-sectional areas with suitable porosity and comparable morphology. Given the evaporation rate differences between the

solvents used, the solvent-polymer interaction may be altered through thermodynamic means during evaporation and this may affect scaffold morphology when THF was used.

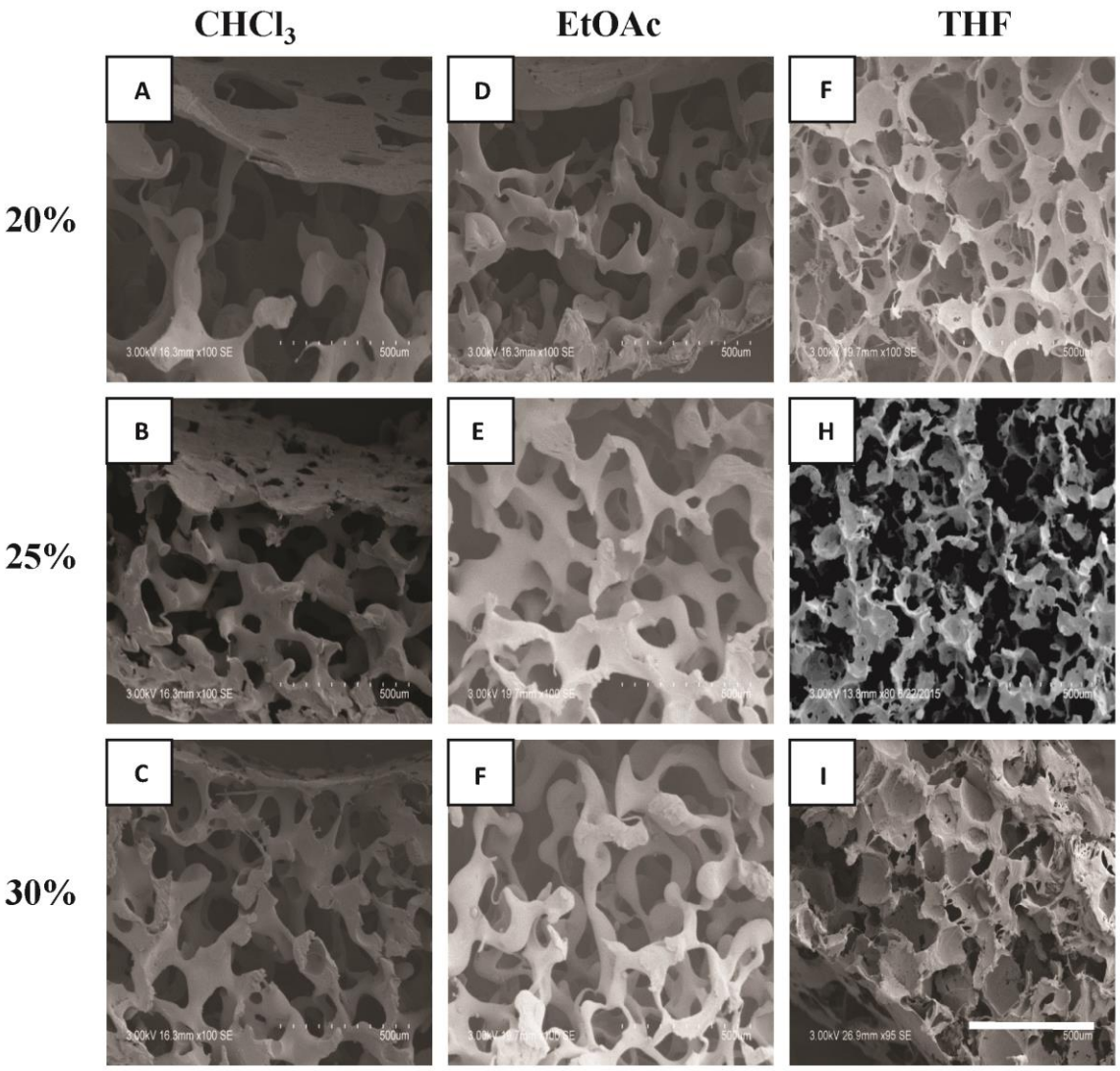

Figure 4.3: SEM cross-sectional images of 20-30% w/w PCL tubular scaffolds fabricated using SCPL. PCL was dissolved in CHCl3 (A-C); EtOAc (D-F) and THF (G-I). Scale bar represents 500 μm.

4.1.3 Micro-CT analysis of 3-D Scaffolds

Since SEM is a qualitative technique, micro-computed tomography (micro-CT), which is a non-destructive and quantitative imaging technique[156], was used. Representative micro-

CT images and the quantification of scaffold morphology and features are presented in Figure 4.4 and Table 4.2 respectively.

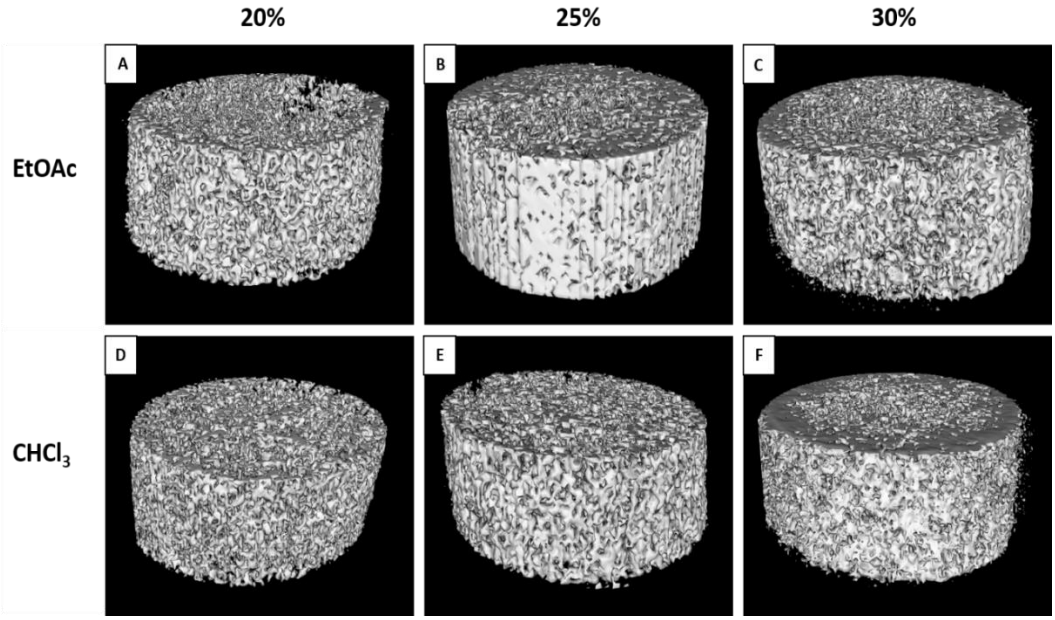

Figure 4.4: Micro-CT images of PCL scaffolds fabricated by dissolving in either CHCl3 or EtOAc at varying w/w concentrations. A-C. PCL dissolved in CHCl3. D-F. PCL dissolved in EtOAc. The images are specific volume elements representing the cross-section within the scaffolds. The white within the image represents PCL and the grey regions represent the pores.

Table 4.2: Micro-CT analysis of 3-D PCL scaffolds at varying w/w concentrations dissolved in either $CHCl_3$ or EtOAc. Two different scaffolds were fabricated and three random measurements were taken for each scaffold (n = 6).

Solvent	PCL Concentration (w/w)	Surface Area to Volume Ratio (mm^{-1})	Strut Thickness (μm)	Pore Diameter (μm)	Overall Porosity (%)
EtOAc	20%	68.4±1.81	29.3±0.835	133±29.0	80.7±1.83
	25%	63.9±6.85	31.5±3.43	137±7.88	81.1±2.72
	30%	65.1±1.75	30.8±0.853	99.7±20.2	76.1±3.31
$CHCl_3$	20%	53.6±0.114	37.4±0.0540	255±1.69	87.1±0.250
	25%	55.9±1.27	35.8±0.811	123±0.348	77.4±0.474
	30%	49.3±1.67	40.6±1.34	107±8.69	72.5±2.25

The effect of both polymer concentration and solvent used were determined by assessing the overall porosity, strut thickness, surface area to volume ratio, and pore size. The need to determine the scaffold parameters was based on the fact that the scaffold architecture is related to not only the mechanical properties of the scaffold but also to the manner in which cells would interact with the scaffold upon seeding.[156] All the scaffolds have sufficient porosity (72% – 87%) suitable for cell seeding and infiltration and were within the range of porosities that are often considered as ideal.[157] There is a clear trend that increasing PCL concentration led to lower scaffold porosity and strut thickness which were expected. The surface area to volume ratio of the scaffolds appeared to be dependent on the type of solvent used instead of the PCL concentration where by scaffolds fabricated using EtOAc had higher surface area to volume ratio than those fabricated using $CHCl_3$. It is known that for a scaffold needs to be highly porous while possessing a high surface area to volume ratio to allow for suitable cell attachment and spreading.[158] Surprisingly the pore diameters obtained from micro-CT measurements were much lower than the particle size of the porogens used (180 – 212 microns). This was not anticipated and the scaffold pore sizes may be underestimated by the micro-CT measurements since NH_4Cl particles are insoluble in the organic solvents to explain size reduction during the scaffold fabrication process. Based on overall scaffold features shown in Table 4.2, scaffolds fabricated from 30% PCL in EtOAc were chosen for subsequent cell culture studies.

4.2 Assessing Cell Viability and Proliferation

Cell viability was evaluated using two cell types: NIH-3T3 fibroblasts and hcSMCs. NIH-3T3 fibroblasts were cultured on either 20%, 25%, or 30% PCL porous scaffolds for 4 or

7 days in 96-well plates. The cells were seeded at 9 x 10^5 cells/scaffold and cultured without additional biochemical factors. NIH-3T3 cells are known to proliferate faster than primary cells[159]; thus NIH-3T3 cells could be least impacted by a change in the environment in which they are seeded in and thus an MTT assay over 4 or 7 days would be suitable for an assessment of viability.

As presented in Figure 4.5A, there was no significant difference in NIH-3T3 viability for 4 days and 7 days culture on both 25% and 30% PCL concentrations. However, at a PCL concentration of 20%, there was a significant difference between day 4 and day 7 where cells cultured for 7 days had increased metabolic activity. Furthermore, cells cultured on 30% PCL concentration for 7 days had significantly lower metabolic activity than those cultured at 20% for 7 days. The cell viability assay was repeated on hcSMCs by seeding 4.5x10^5 cells/scaffold. As shown in Figure 4.5B, unlike the NIH-3T3 fibroblasts, the hcSMCs viability increased both with PCL concentration and with increased culture time. Unexpectedly, there appears to be a diverging trend on the metabolic activity the two cell types tested. While NIH-3T3 cells were metabolically more active at 20% PCL concentration, hcSMCs were more active at 30% PCL concentration. Although it remained to be tested, cell spreading and phenotype variation may be one factor.

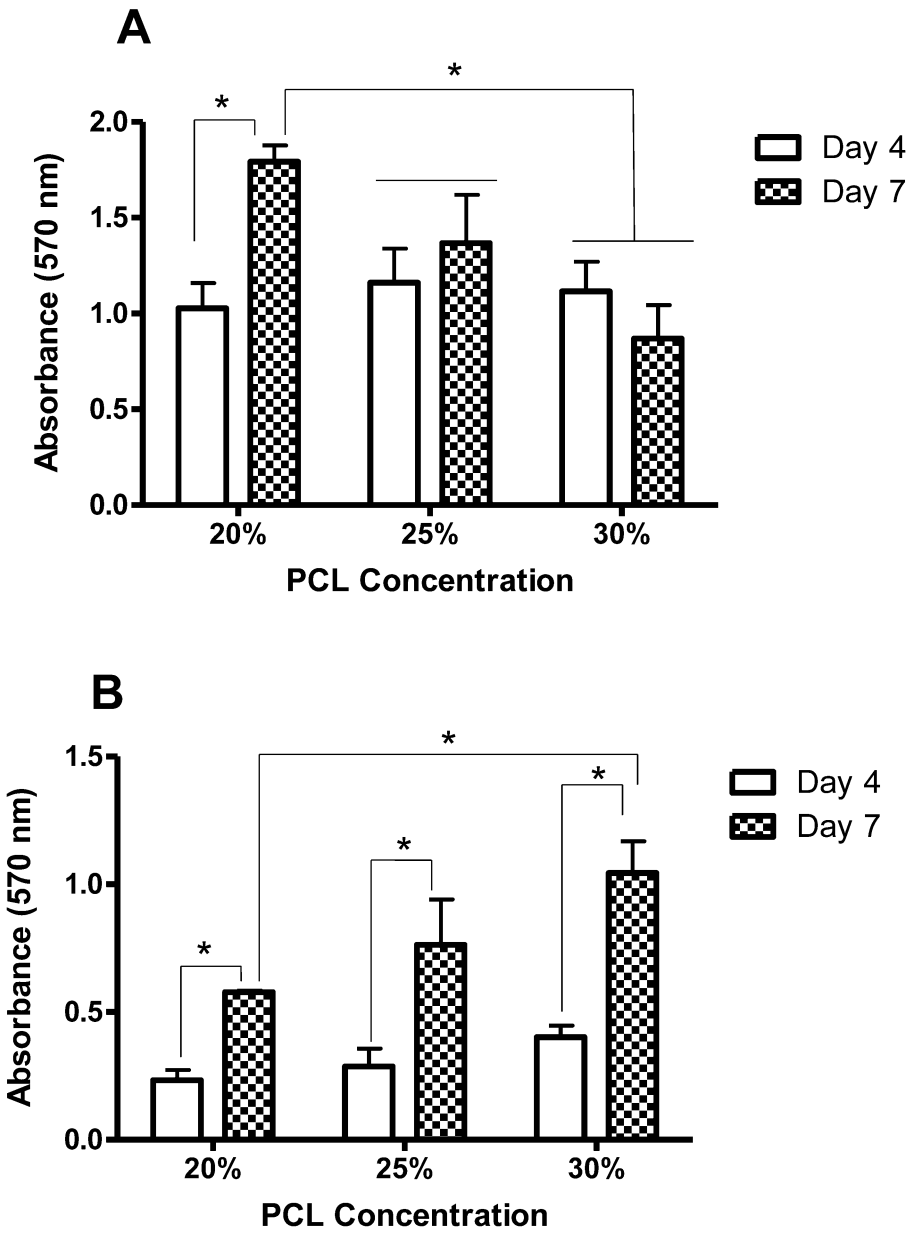

Figure 4.5: MTT assays of NIH-3T3 fibroblasts or hcSMCs on 20%, 25%, or 30% w/w PCL scaffolds dissolved in EtOAc. A: Viability of NIH-3T3 fibroblasts assessed at day 4 and 7. B: Viability of hcSMCs assessed at day 4 and 7. Significance: $p<0.05$ (*).

Varying the scaffold polymer concentration was thought to have a role in influencing the ability of the cells to adhere to the scaffold and proliferate. In hydrogel systems, increasing the polymer concentrations within scaffolds can significantly reduce cell viability.[160]

However, the likely reason to this in hydrogel systems are the higher cross-linking densities which limit the mass transfer characteristics.[161] In electrospinning systems, increasing the polymer concentration can result in a non-linear relationship between solution concentration and fiber diameter whereas increased fibers diameters result in lower viability.[162] However, there was no study found in the literature of cell viability in the SCPL process at various polymer concentrations which is surprising given that scaffold architecture is paramount to cellular behavior.[156]

To evaluate if the increase in viability of the hcSMCs correlated with that of an increase in proliferation, DNA quantification was conducted. It is known that an MTT metabolic assay does not always parallel observations seen in the more quantitative DNA assay in 3-D cultures.[163] As the 30% PCL concentration showed significantly higher hcSMCs viability, it was chosen to for cell proliferation study. The proliferation of the hcSMCs seeded on the 30% PCL concentration at days 4 and 7 is shown in Figure 4.6. By day 7, the cell number was significantly higher than day 4, confirming the trend suggested by the MTT data and ability of the 30% PCL scaffolds to support and promote proliferation over time. Considering both the MTT and DNA quantification data, the 30% PCL scaffolds prepared in EtOAc were deemed to support cell viability and growth over time most optimally and were utilized in subsequent cell culture experiments.

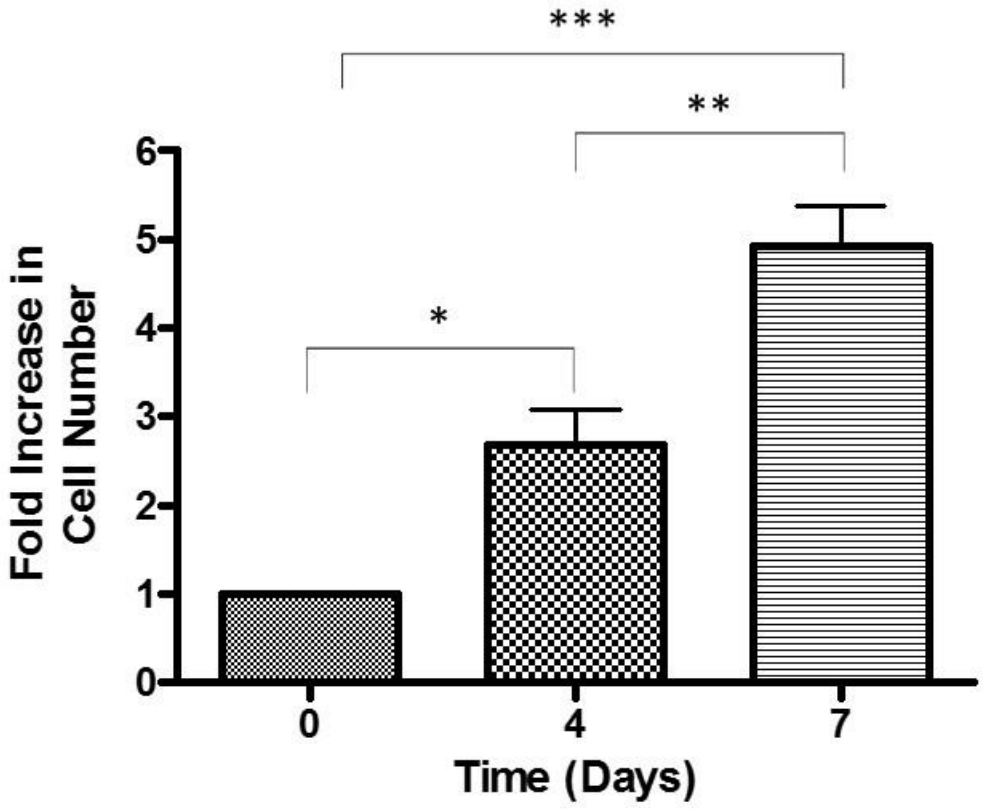

Figure 4.6: DNA quantification of hcSMCs seeded onto 30% w/w PCL scaffolds at days 4 and 7. Significance: $p<0.05$ (*), $p<0.01$ (**), $p<0.001$ (***).

4.3 The Effect of atRA on Cultured Smooth Muscle Cells

4.3.1 Cell Morphological Response to atRA Treatment

Before studying the effect was atRA on elastin expression on PCL scaffolds, it was thought that any potential toxic effects that atRA may have on the hcSMCs should be explored. While most studies occurred in 2-D cultures, one prior study investigated atRA treatment on vSMCs in 3-D culture using aortic SMCs.[138] In a direct comparison with non-coronary medial SMCs, it was found that hcSMCs may differ in gene expression and response to biochemical factor treatment in culture.[164] Additionally, it is known that the response to factors can vary between 2-D and 3-D microenvironments. Lin *et al*. demonstrated that

hcSMCs can vary in their response to TGF-β1, with a more pronounced elastogenic response in 3-D than 2-D culture.[111] Since there are no prior studies about the effect of atRA on the viability of hcSMCs seeded onto 3-D porous scaffolds, it seemed reasonable to assess its suitability. In order to have a clean system that does not confound results, a non-degradable polyurethane scaffold was fabricated in the same way as the PCL scaffolds. There are no degradation products in this polyurethane (at least in the short term); thus cell phenotype will not be affected and does not confound results as per previous publications from Mequanint's lab [111, 139, 149, 158, 165, 166]. There is little difference between the model polyurethane scaffold and PCL in terms of hydrophobicity indicating that cells would not significantly favor one polymer over the other for cell adhesion. Additionally, both were pre-conditioned in buffer which has been shown to increase the hydrophilicity of the polymers and improve cell viability.[167]

100 μM of atRA concentration was added to hcSMCs seeded on porous polyurethane scaffolds and confocal images were taken after culturing for 4 and 7 days. The confocal images presented in Figure 4.7 revealed that hcSMCs formed a dense layer surrounding the scaffold struts with no indication of cytoskeletal or DNA fragmentation. At day 7, cells were observed bridging the scaffold pores suggesting active migration.

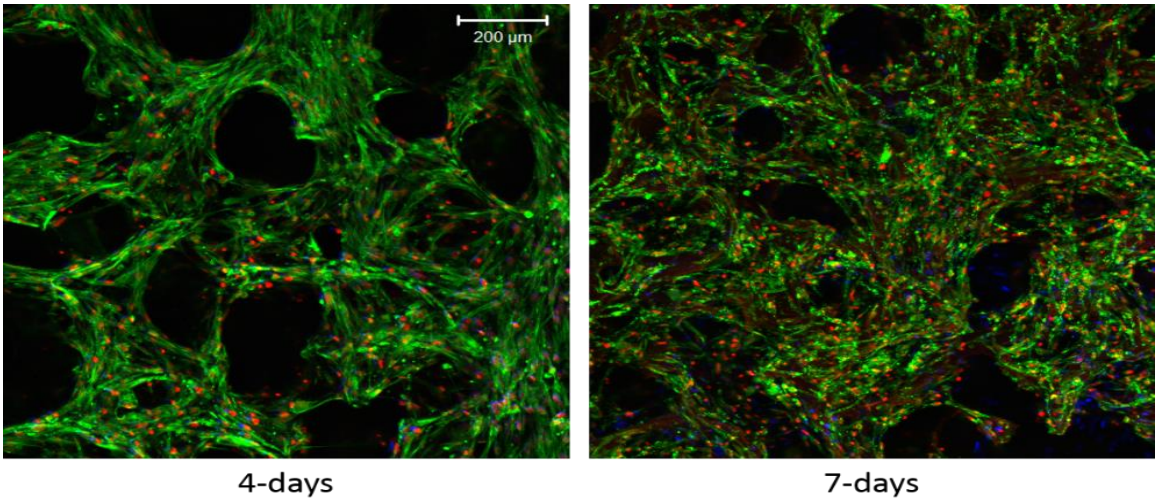

Figure 4.7: Confocal images of hcSMCs seeded onto porous 3-D polyurethane scaffolds and exposed to 100 µM of atRA. Confocal images were taken after 4 and 7 days of culture. Scale bar represents 200 µm. Staining: F-actin (green) and DAPI (red).

While 100 µM of atRA appeared to support growth and suitable spreading by day 7, the effect of fibronectin coating and cultures longer than 7 days were studied. The rationale for fibronectin coating was that, it is a frequently used ECM component to enhance cell attachment and spreading on scaffolds through its RGD motif that can facilitate integrin binding.[168, 169] There are many studies that utilize fibronectin to increase cellular attachments to scaffolds to accelerate favorable cell-scaffold interactions.[169-171] The rationale for longer time culture (14 days) was that cells may respond differently to sustained atRA treatment compared to shorter times. Figure 4.8 displays confocal images of hcSMCs at day 14 on the porous 3-D model polyurethane scaffold. While cells were observed spreading on the fibronectin-coated scaffolds with abundant F-actin, the treatment of cells with 150 µM atRA resulted in diminished F-actin suggesting cell death. It is suggested that atRA can increase the expression of β1-integrin which can interact strongly with fibronectin.[172]

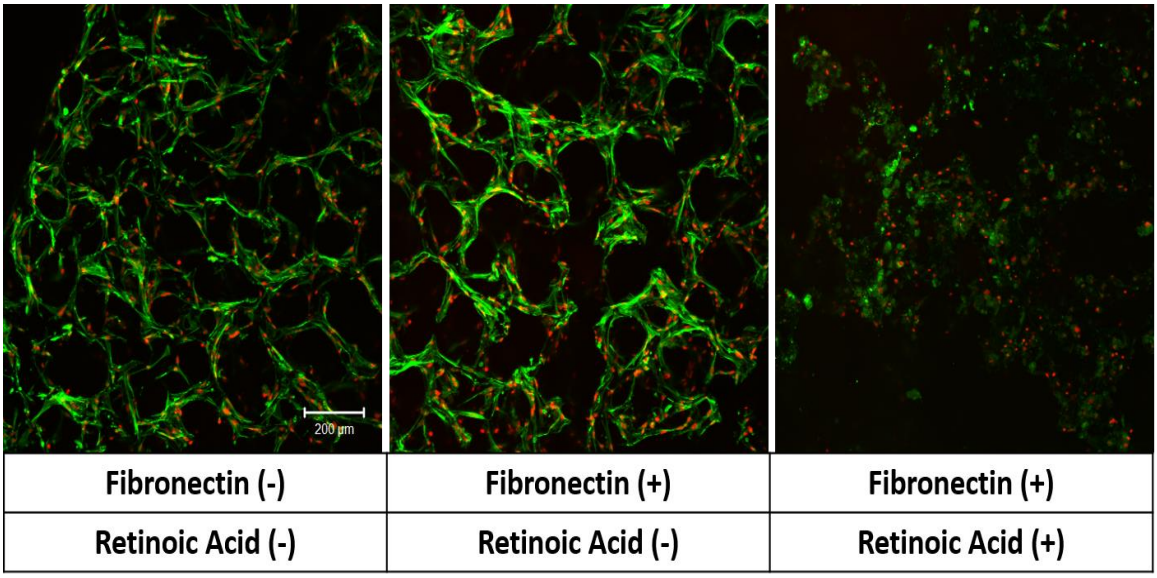

Figure 4.8: Confocal images of hcSMCs seeded on a porous 3-D polyurethane scaffold with or without fibronectin pre-treatment and 150 µM atRA. Cells were cultured for 14 days before fixation and confocal imaging. Scale bar represents 200 µm. Staining: F-actin (green) and DAPI (red).

It is worthy to note that cells had similar morphology and density regardless of fibronectin treatment. In view of this and since fibronectin may play a role in influencing elastin synthesis by shifting vSMCs into a more synthetic phenotype [173], its presence may further confound the effect of atRA and therefore, was precluded from further studies. Grenier *et al*.[166] found that when hcSMCs were cultured on fibronectin coated porous 3-D scaffolds, the expression of vSMC contractile phenotypic markers was reduced. As elastogenesis is known to likely be enhanced in the synthetic state, fibronectin may influence the way in which cells respond to biochemical factor stimulation in the context of elastin expression. While the design of the current study was focused on assessing differences between 2-D and 3-D microenvironments and how cell responses will vary to biochemical factor exposure, future studies may investigate the impact that various coatings would have on elastogenesis. While Grenier *et al*.[166] focused on fibronectin and Matrigel coatings, that

study did not assess elastin at the transcriptional or translational level. The impact of understanding how coating with ECM proteins could increase elastogenesis may be invaluable for future experimental designs attempting to augment elastogenesis for VTE.

4.3.2 The effect of atRA Concentration on Elastin Gene Expression

The concentration of atRA may affect tropoelastin transcription in a dose-dependent manner. To test this, hcSMCs were seeded in 2-D culture plates and were treated with different concentrations of atRA (0.1 to 10 μM) over 4 days culture. While it can be expected that the elastogenic effect of atRA may vary temporally, the response to varying concentrations should be consistent with time. As shown in Figure 4.9, the concentration that promoted the highest fold increase in tropoelastin transcription occurred when using 10 μM atRA; producing a 2-fold increase in gene expression. While 0.1 and 1 μM atRA also increased tropoelastin mRNA levels compared to the untreated control, the fold increase was not significant. Based on the observations of Figures 4.7 and 4.8, it was tempting to increase the atRA concentration to boost elastin in the gene expression study. Although 100 μM and 150 μM were investigated for the confocal studies, these concentrations are not physiological and may have other negative effects beyond boosting elastin expression. Therefore, it was decided to limit the gene/protein expression studies to reported physiological atRA concentration ranges.[113] Not withstanding this, higher concentration of atRA would be tolerated *in vivo*, as documented for acute promyelocytic leukemia chemotherapy.[174] *In vitro* studies suggested that utilizing higher atRA concentrations would result in a decrease in vSMC proliferative ability which emphasized

the need to select a lower concentration while still facilitating the highest increase in tropoelastin transcriptional activity.[123, 175]

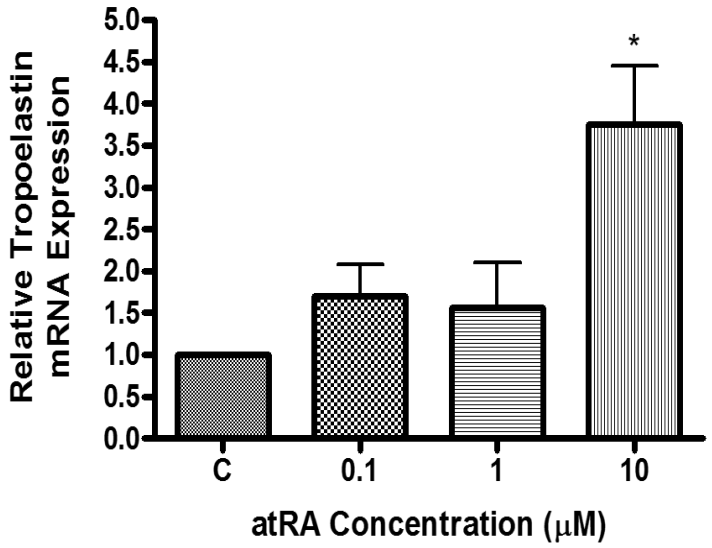

Figure 4.9: The effect of atRA concentration on tropoelastin gene expression in hcSMCs cultured on 2D plates for 4 days. 10 μM atRA produced the highest tropoelastin fold increase and was utilized for subsequent experiments. Significance: $p<0.05$ (*) was observed for 10 μM of atRA compared to the untreated control (C) and 0.1 and 1 μM of atRA.

4.4 The Effect of AA and atRA Combination on Tropoelastin Synthesis

As the concentration of atRA in gene expression experiments was maximum at 10 μM, the effect on tropoelastin protein expression due to a combined treatment of AA and atRA was investigated. Although AA has been reported to decrease elastogenesis in 2-D cultures[137], the rationale behind the biochemical factor's use was to increase collagen expression[136, 137] since both elastin and collagen are essential ECM components of a vascular tissue. Thus, as atRA has been reported to increase elastin [133], it was necessary to investigate the interaction between the two biochemical factors. However, there have been limited studies

investigating the effect of the combination of AA and atRA on elastogenesis in hcSMCs with the work by Ogle *et al*. being the lone consideration.[138] Ideally, the ability to increase elastin with combined biochemical factor treatment would enhance vascular tissue fabrication. Thus, the premise of the investigation was that while atRA and AA would show an increase and decrease in elastin expression respectively, it was unknown to what effect the combination would have. To test this, a time-course experiment (24 hours – 96 hours) was conducted in 2-D culture plates after the cells had reached confluence. The reason for reaching cell confluency before biochemical factors treatment was to limit the effect of phenotypic modulation in culture.[24]

As shown in Figure 4.10, the increased tropoelastin expression when supplemented with atRA was significantly higher at all time points relative to AA alone. Conversely, AA decreased elastin expression compared with atRA alone at all time-points. The combined AA and atRA treatment significantly decreased tropoelastin synthesis at all time points. This suggested that the effect of the combination was influenced to a greater extent by AA as no significant differences were observed between AA and the combination at the tested time-points while significance occurred between atRA alone and the combined treatment. It was suspected that AA may be exerting its effects at an earlier stage of tropoelastin synthesis whereas atRA functions at a later stage. For instance, studies suggested that atRA may influence tropoelastin mRNA stability while it is known that AA may exert its effect earlier, directly at the transcriptional level.[137]

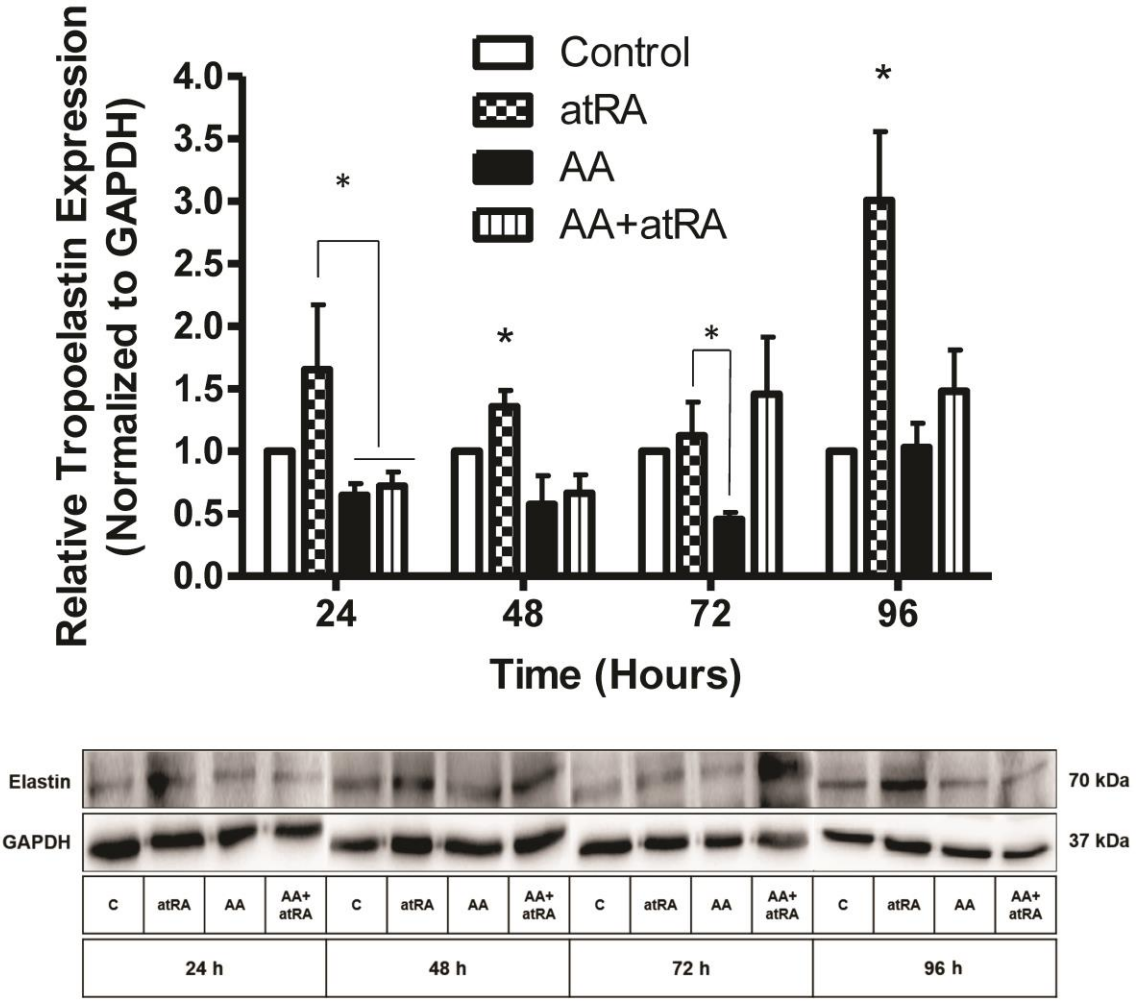

Figure 4.10: Time-course evaluation tropoelastin synthesis (as determined by Western blot) isolated from whole-cell lysates of hcSMCs in response to various biochemical factor treatments. Data are normalized to GAPDH and a control without biochemical factor treatment. Significance: $p<0.05$ (*) was observed as indicated in the graph.

It seems likely that less tropoelastin mRNA may be produced for the atRA to stabilize which may account for the similar protein expression patterns generally observed between AA and the combination treatment. To evaluate this possibility, tropoelastin transcription experiments at 48, 72, and 96 hours were conducted. As shown in Figure 4.11 the tropoelastin mRNA expression levels were not significantly different compared with the control at 72 and 96 hours, which correlated with the protein expression levels seen in

Figure 4.10. However, there was a significant increase (5.5-fold increase) at the 48 hour time point. Taken together, this may suggest that while temporal variation exists in terms of transcriptional activity, the effect of the decrease in tropoelastin protein expression with combined atRA and AA treatment is very likely attributed to transcriptional repression.

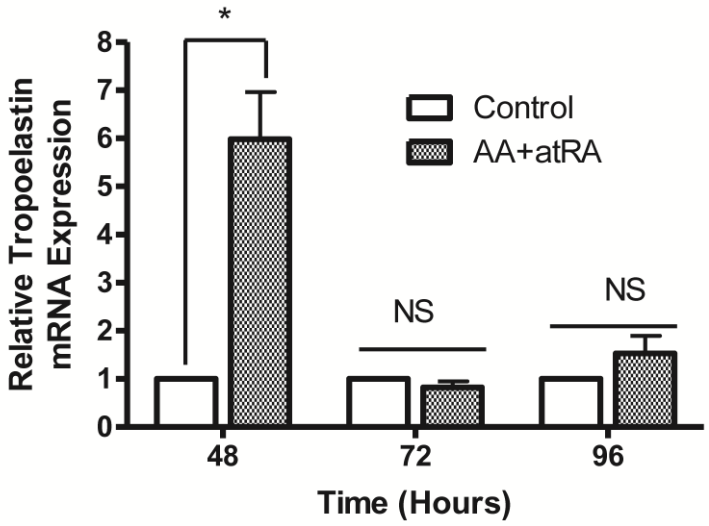

Figure 4.11: qPCR assessing tropoelastin transcription in hcSMCs at 48, 72, and 96 hours comparing a combination of AA and atRA to a non-treated control, both normalized to GAPDH. Significance: $p<0.05$ (*) was observed for the combination treatment relative to the untreated control at the 48-hour time point. NS: Not significant.

4.5 Comparative Study of Elastin Synthesis in 2D Plates and 3D PCL Scaffolds

4.5.1 Spatial Effects on Elastin Synthesis

The effect of the culture microenvironment on elastin synthesis was evalauted at days 4 and 7 by seeding the hcSMCs onto 2-D culture plates and 3-D porous PCL scaffolds. Elastin expression at days 4 and 7 in 2-D and 3-D cultures is shown in Figure 4.12.

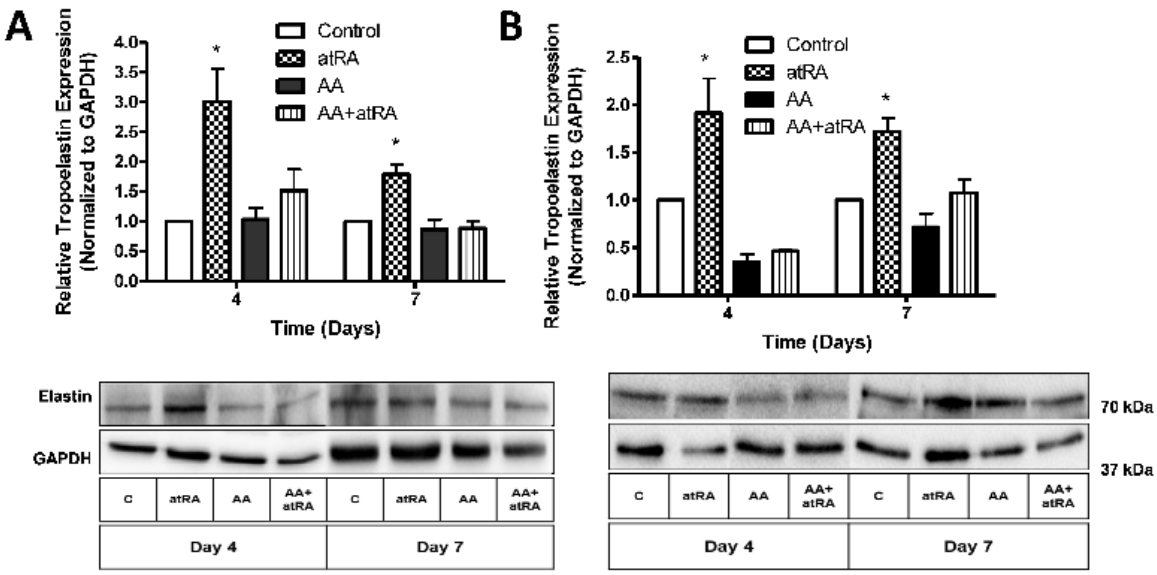

Figure 4.12: Western blotting of whole-cell lysates of hcSMCs assessing for tropoelastin expression in response to biochemical factor treatment in 2D culture plates (A) and 3D PCL scaffolds (B). Data was normalized to GAPDH and a non-treated control. Significance: $p<0.05$ (*).

Two observations can be made from Figure 4.12: (i) The protein expression levels had similar patterns between 2-D and 3-D, and (ii) similar to short culture times (Figure 4.10), the combined treatment reduced elastin expression in 3-D. This suggests that although the cells are seeded in different environments, the effects of the biochemical factor stimulation on elastin expression are not spatially dependent. Notwithstanding this, the amount of elastin produced was more pronounced in 3-D. This is consistent with work by Lin *et al*.[111] who suggested that the 3-D environment alone is sufficient to increase elastin expression relative to 2-D cultures. However, the effect of AA in 3-D cultures appears to be low compared to 2-D cultures at day 4. By day 7, the lowering of elastin protein expression in response to AA treatment or a combination with atRA was alleviated and rose to levels similar to those seen in the non-treated controls. While the experimental time-point ended at day 7, it would be interesting to study if the reduction seen in 3-D compared to atRA

alone would be overcome at longer time-points. Previous work by Ogle *et al*. [138] examining the combination treatment in 3-D did not investigate the impact of atRA or AA alone on elastin protein expression in 3-D and thus it is difficult to make direct comparison.

4.5.2 Combinational Approach to Rescue Elastin Expression in 3-D Culture

The decrease in elastin protein expression with the combination treatment compared to that of atRA alone was unfortunate as both factors are required for either increasing collagen or elastin and are thus necessary for engineering viable vascular tissues. As the experiments in both 2-D and 3-D suggested that AA was lowering elastin synthesis, a new approach was devised. To maintain the elastogenic effect of atRA while preserving the ability of AA to increase collagen expression, a sequential treatment was attempted. AA was initially supplemented to increase collagen expression prior to stopping AA stimulation and providing atRA treatment. This was implemented to test if elastin expression can be rescued after the expected decrease in response to AA treatment. As Figure 4.13 demonstrates, the effect of AA seemed to have a significant impact on elastin expression even when the AA was removed from the culture environment. Removal of AA for 1 and 3 days did not result in a significant difference compared to the control over the 7 days culture. This suggests that both 1 day and 3 days exposure was not sufficient produce elastin at the level observed when atRA was added alone over 4 day assay (compare Fig 4.13 with Fig 4.10 and 4.12). However, there was a significant difference between AA treatment alone over the 7 days and 3 days of rescue with the atRA. This suggested that the repression on elastin synthesis induced by AA can be overcome by subsequent addition atRA, though it may take longer than 1 day to observe an effect.

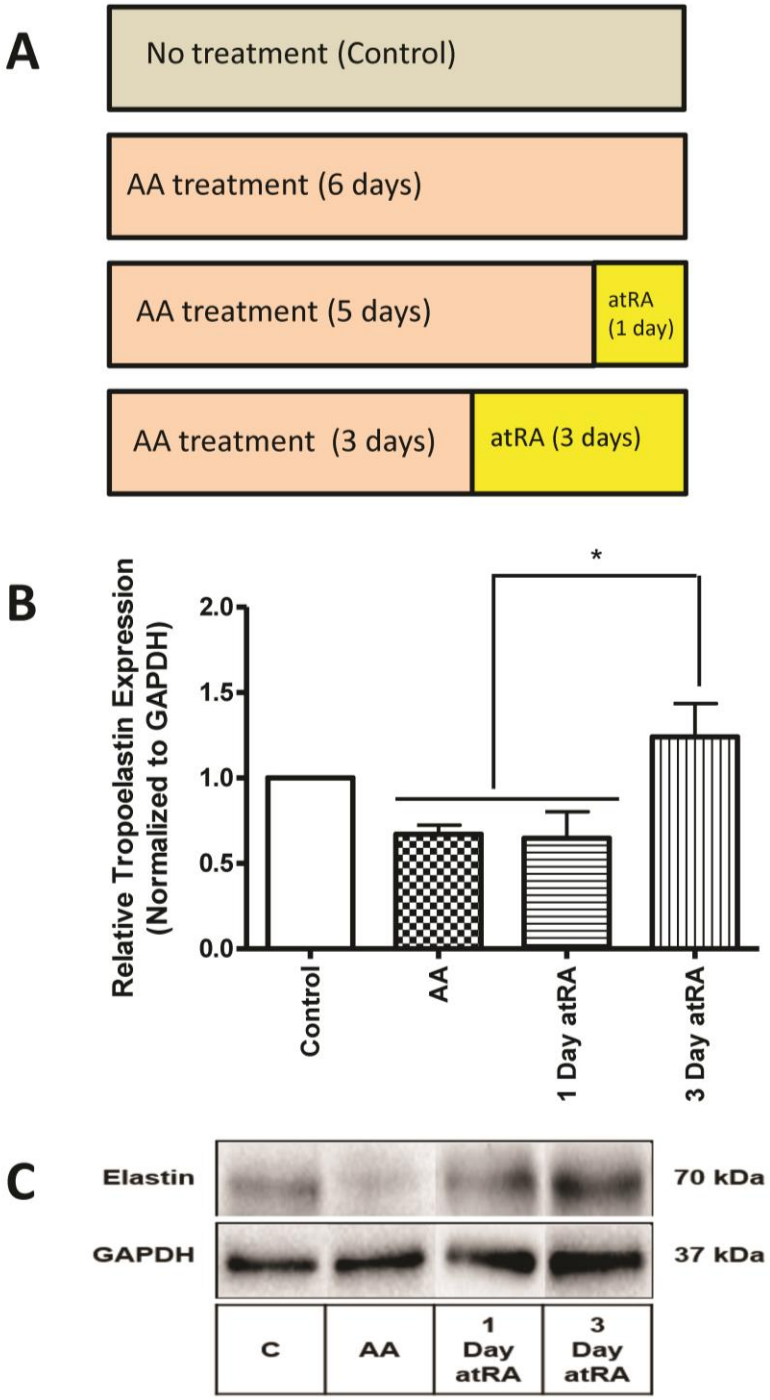

Figure 4.13: Elastin expression assessed by Western blotting of whole-cell lysates of hcSMCs after sequential non-overlapping factor exposure for different times. The schematic of the experimental design is shown in A where cells were cultured either without treatment (control), 6 days of AA treatment, 5 days AA followed by 1 day atRA treatment or 3 days AA followed by 3 days atRA treatment. Cells were harvested on the 7^{th} day for protein extraction and Western blotting. Significance: $p<0.05$ (*) was observed for 3 days of atRA rescue compared to AA alone.

It is possible that the collagen expression stimulated by AA may have suppressed elastin expression and this is plausible. Although collagen gels are commonly utilized in VTE they have been shown to suppress elastogenic effects *in vitro*.[11] Another possibility for this temporal suppression could be that some AA is adsorbed onto the surfaces of the PCL scaffold and acted on the smooth muscle cells for longer times than anticipated. However, given the rapid oxidation of AA in tissue culture environments, this is unlikely.[176] This suggests that AA may have delayed inhibitory effects on elastogenesis. It would be interesting to examine the effect of atRA treatment first followed by AA on elastin and collagen synthesis or using a longer sequential non-overlapping factor exposure to observe if the AA mediated decrease can be mitigated with time.

4.5.3 The Effect of Biochemical Factors on α-SMA Expression

As there is a known correlation with ECM synthesis and vSMC phenotype, the effect of biochemical factor stimulation on the phenotype was investigated in both 2-D and 3-D cultures. However, when assessing vSMC phenotypic plasticity, it is known that there can be significant heterogeneity within a culture, thus making the phenotype difficult to assess.[177] In spite of this, atRA has been shown to induce vSMCs to progress to a more contractile phenotype in 2-D.[118, 119] There is no data on the effect that AA may have on vSMC phenotype in 3-D cultures. As AA reduced elastin protein expression at both day 4 and day 7, the role of AA in cell phenotype was investigated (Figure 4.14). While there are numerous contractile protein markers, α-SMA is associated with an earlier/mid stage differentiation marker was chosen in comparison to the more mature markers such as

smooth muscle myosin-heavy chain which occur at later time-points.[105] It was thought that α-SMA would indicate the onset of transition to the contractile phenotype.

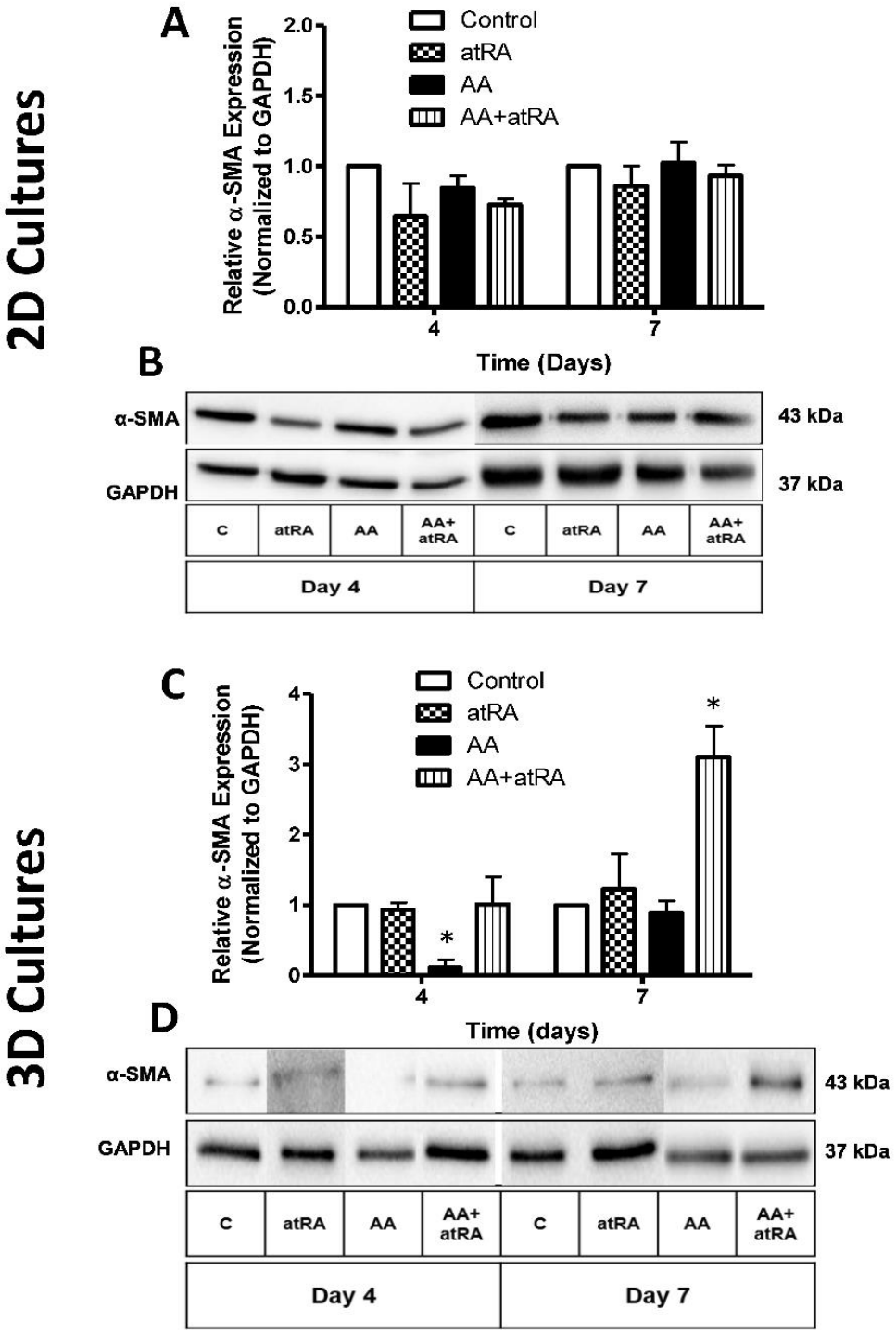

Figure 4.14: Western blotting of whole-cell lysates of hcSMCs assessing for α-SMA normalized to GAPDH at day 4 and day 7 cultures for 2D cultures (A, B) and 3D cultures (C, D). Significance: $p<0.05$ (*).

In 2-D, α-SMA expression levels were similar across treatment groups at both day 4 and day 7; however, α-SMA expression was significantly higher on the 3-D combination treated cultures at day 7 than all other treatments. This suggests that elastin expression in 2-D may be independent from the adoption of a contractile phenotype when treated with AA alone or in combination with atRA. Moreover, the lack of significance for all biochemical factor treatments relative to the controls at both day 4 and day 7 indicates that in 2-D these biochemical factors possess little phenotypic influence compared to the seeding environment alone. Generally stiffer substrates induce a more synthetic phenotype.[106] It appears that AA or the combination treatment have no effect on α-SMA expression in both 2-D and 3-D cultures to induce the contractile phenotype. As atRA was expected to promote the contractile state, in 2-D, the AA mediated influence on low elastin expression appears to be potentially dependent on phenotype. The current data is consistent with a study conducted by Ryan *et al*.[178] who suggested that in collagen gels, insoluble elastin can induce a contractile phenotype characterized by an increase in α-SMA.

Chapter 5 – Conclusions and Future Directions

5.1 Conclusions

The present study assessed the SCPL process for PCL scaffold fabrication. The scaffolds were then utilized for culturing smooth muscle cells with biochemical factors to enhance elastin synthesis. The initial scaffold fabrication considered PCL dissolved in varying concentrations and solvents. It was found that a hold time of 2 hours in the glass rod produced the best scaffolds as shorter times led to disintegration and longer times resulted in an inability to remove the scaffold from the glass tube casing irrespective of solvent chosen and concentration of PCL. However, the type of the solvent was found to influence the morphology of the scaffolds. SEM studies showed that THF produced scaffolds that have poorly-interconnected and closed pores. In tubular scaffolds, all solvents produced bubble-like films on the ablumen and isolated pores in the lumen regardless of the PCL concentration. Micro-CT was used to identify EtOAc as the best solvent to fabricate the PCL scaffolds based on overall porosity, strut thickness, and surface area to volume ratio. Given the higher ratios obtained with EtOAc as the solvent, it was used in the scaffold fabrication for subsequent cell culture studies. MTT assay using NIH-3T3 fibroblasts and hcSMCs on PCL scaffolds fabricated from 20, 25, 30% concentration showed an opposite trend as a function of PCL used to fabricate the scaffolds likely due to differences in metabolic activity and proliferation rate between the two cell lines. While 30% resulted in significantly less viability than seen with 20% for the NIH-3T3 fibroblasts, 30% promoted the highest viability with hcSMCs which was confirmed with a more quantitative DNA

assay. Given the higher viability and proliferation observed with the hcSMCs and as the 30% PCL concentration was more mechanically stable, it was chosen for elastogenic studies. qPCR confirmed that 10 μM atRA promoted the highest tropoelastin transcriptional activity and confocal imaging on model polyurethane scaffolds indicated that higher concentrations at day 4 and 7 produced no cytotoxic effects. To evaluate the effect of AA and atRA, Western blotting of whole-cell lysates for tropoelastin was conducted. Significant increases in relative expression when treated with atRA alone occurred at 48 and 96 hours indicating that temporal variation exists in the elastogenic effect of atRA. However, the combination of AA and atRA expression more closely mirrored that of AA alone which indicated that AA may have a greater effect than atRA in 2-D cultures. Similar trends were observed when comparing tropoelastin expression in 2-D culture plates and 3-D PCL scaffolds, with atRA treatment alone significantly increasing expression compared to AA alone or the combination at both day 4 and day 7 in 3-D and day 7 in 2-D. Interestingly, when assessing whether this trend correlated with the phenotype of the hcSMCs in both 2-D and 3-D it was found that α-SMA remained constant in 2-D yet was increased over time with AA alone and the combination treatment. Given the decrease in elastin when combination treatment was used, a sequential treatment was shown to be effective to enhance elastin synthesis. Overall, the study in this thesis provided insights into early responses of hcSMCs on SCPL PCL scaffolds and elastin synthesis in response to atRA and AA.

5.2 Future Directions

Moving forward, the following future studies are suggested:

- Conduct long-term cultures using the sequential addition of biochemical factors.
- Combine biochemical factors with biomechanical forces to study the possible synergy between them
- Understand molecular mechanisms of elastin synthesis in response to atRA in 3-D cultures.

6. References

[1] N.J. Pagidipati, T.A. Gaziano, Estimating deaths from cardiovascular disease: a review of global methodologies of mortality measurement, Circulation 127(6) (2013) 749-56.

[2] J. Jin, G.E. Sklar, V. Min Sen Oh, S. Chuen Li, Factors affecting therapeutic compliance: A review from the patient's perspective, Ther Clin Risk Manag 4(1) (2008) 269-86.

[3] S. Pashneh-Tala, S. MacNeil, F. Claeyssens, The Tissue-Engineered Vascular Graft-Past, Present, and Future, Tissue Eng Part B Rev (2015).

[4] P.J. Wiegman, W.L. Barry, J.A. McPherson, C.A. McNamara, L.W. Gimple, J.M. Sanders, G.G. Bishop, E.R. Powers, M. Ragosta, G.K. Owens, I.J. Sarembock, All-trans-retinoic acid limits restenosis after balloon angioplasty in the focally atherosclerotic rabbit : a favorable effect on vessel remodeling, Arterioscler Thromb Vasc Biol 20(1) (2000) 89-95.

[5] J.E. Wagenseil, R.P. Mecham, Vascular extracellular matrix and arterial mechanics, Physiol Rev 89(3) (2009) 957-89.

[6] G.G. Belz, Elastic properties and Windkessel function of the human aorta, Cardiovasc Drugs Ther 9(1) (1995) 73-83.

[7] R.K. Jain, Molecular regulation of vessel maturation, Nat Med 9(6) (2003) 685-93.

[8] A.V. Kamenskiy, Y.A. Dzenis, J.N. MacTaggart, T.G. Lynch, S.A. Jaffar Kazmi, Pipinos, II, Nonlinear mechanical behavior of the human common, external, and internal carotid arteries in vivo, J Surg Res 176(1) (2012) 329-36.

[9] N. Thottappillil, P.D. Nair, Scaffolds in vascular regeneration: current status, Vasc Health Risk Manag 11 (2015) 79-91.

[10] S.L. Sandow, D.J. Gzik, R.M. Lee, Arterial internal elastic lamina holes: relationship to function?, J Anat 214(2) (2009) 258-66.

[11] A. Patel, B. Fine, M. Sandig, K. Mequanint, Elastin biosynthesis: The missing link in tissue-engineered blood vessels, Cardiovasc Res 71(1) (2006) 40-9.

[12] G.A. Holzapfel, H.W. Weizsacker, Biomechanical behavior of the arterial wall and its numerical characterization, Comput Biol Med 28(4) (1998) 377-92.

[13] A.G. Vouyouka, B.J. Pfeiffer, T.K. Liem, T.A. Taylor, J. Mudaliar, C.L. Phillips, The role of type I collagen in aortic wall strength with a homotrimeric, J Vasc Surg 33(6) (2001) 1263-70.

[14] A. Bigi, A. Ripamonti, N. Roveri, X-ray diffraction and scanning electron microscopy of bovine media aortic wall, Connect Tissue Res 5(1) (1977) 37-9.

[15] A.P. Ebrahimi, Mechanical properties of normal and diseased cerebrovascular system, J Vasc Interv Neurol 2(2) (2009) 155-62.

[16] M.J. Chow, R. Turcotte, C.P. Lin, Y. Zhang, Arterial extracellular matrix: a mechanobiological study of the contributions and interactions of elastin and collagen, Biophys J 106(12) (2014) 2684-92.

[17] J.E. Wagenseil, R.P. Mecham, New insights into elastic fiber assembly, Birth Defects Res C Embryo Today 81(4) (2007) 229-40.

[18] D.V. Bax, U.R. Rodgers, M.M. Bilek, A.S. Weiss, Cell adhesion to tropoelastin is mediated via the C-terminal GRKRK motif and integrin alphaVbeta3, J Biol Chem 284(42) (2009) 28616-23.

[19] D.J. Johnson, P. Robson, Y. Hew, F.W. Keeley, Decreased elastin synthesis in normal development and in long-term aortic organ and cell cultures is related to rapid and selective destabilization of mRNA for elastin, Circ Res 77(6) (1995) 1107-13.

[20] M.H. Swee, W.C. Parks, R.A. Pierce, Developmental regulation of elastin production. Expression of tropoelastin pre-mRNA persists after down-regulation of steady-state mRNA levels, J Biol Chem 270(25) (1995) 14899-906.

[21] J. Uitto, S. Hsu-Wong, S.D. Katchman, M.M. Bashir, J. Rosenbloom, Skin elastic fibres: regulation of human elastin promoter activity in transgenic mice, Ciba Found Symp 192 (1995) 237-53; discussion 253-8.

[22] H. Umeda, M. Aikawa, P. Libby, Liberation of desmosine and isodesmosine as amino acids from insoluble elastin by elastolytic proteases, Biochem Biophys Res Commun 411(2) (2011) 281-6.

[23] M.J. Rock, S.A. Cain, L.J. Freeman, A. Morgan, K. Mellody, A. Marson, C.A. Shuttleworth, A.S. Weiss, C.M. Kielty, Molecular basis of elastic fiber formation. Critical interactions and a tropoelastin-fibrillin-1 cross-link, J Biol Chem 279(22) (2004) 23748-58.

[24] Y. Cao, Y.F. Poon, J. Feng, S. Rayatpisheh, V. Chan, M.B. Chan-Park, Regulating orientation and phenotype of primary vascular smooth muscle cells by biodegradable films patterned with arrays of microchannels and discontinuous microwalls, Biomaterials 31(24) (2010) 6228-38.

[25] S. Kyle, A. Aggeli, E. Ingham, M.J. McPherson, Production of self-assembling biomaterials for tissue engineering, Trends Biotechnol 27(7) (2009) 423-33.

[26] L. Cardamone, A. Valentin, J.F. Eberth, J.D. Humphrey, Origin of axial prestretch and residual stress in arteries, Biomech Model Mechanobiol 8(6) (2009) 431-46.

[27] C.A. Taylor, J.D. Humphrey, Open Problems in Computational Vascular Biomechanics: Hemodynamics and Arterial Wall Mechanics, Comput Methods Appl Mech Eng 198(45-46) (2009) 3514-3523.

[28] T.R. Cox, J.T. Erler, Remodeling and homeostasis of the extracellular matrix: implications for fibrotic diseases and cancer, Dis Model Mech 4(2) (2011) 165-78.

[29] M. Loukas, A. Sharma, C. Blaak, E. Sorenson, A. Mian, The clinical anatomy of the coronary arteries, J Cardiovasc Transl Res 6(2) (2013) 197-207.

[30] J.T. Dodge, Jr., B.G. Brown, E.L. Bolson, H.T. Dodge, Lumen diameter of normal human coronary arteries. Influence of age, sex, anatomic variation, and left ventricular hypertrophy or dilation, Circulation 86(1) (1992) 232-46.

[31] I. Ozolanta, G. Tetere, B. Purinya, V. Kasyanov, Changes in the mechanical properties, biochemical contents and wall structure of the human coronary arteries with age and sex, Med Eng Phys 20(7) (1998) 523-33.

[32] A.K. Hiteshi, D. Li, Y. Gao, A. Chen, F. Flores, S.S. Mao, M.J. Budoff, Gender differences in coronary artery diameter are not related to body habitus or left ventricular mass, Clin Cardiol 37(10) (2014) 605-9.

[33] C.V. Bouten, P.Y. Dankers, A. Driessen-Mol, S. Pedron, A.M. Brizard, F.P. Baaijens, Substrates for cardiovascular tissue engineering, Adv Drug Deliv Rev 63(4-5) (2011) 221-41.

[34] C.J. van Andel, P.V. Pistecky, C. Borst, Mechanical properties of porcine and human arteries: implications for coronary anastomotic connectors, Ann Thorac Surg 76(1) (2003) 58-64; discussion 64-5.

[35] G. Heusch, Heart rate in the pathophysiology of coronary blood flow and myocardial ischaemia: benefit from selective bradycardic agents, Br J Pharmacol 153(8) (2008) 1589-601.

[36] D. Mozaffarian, E.J. Benjamin, A.S. Go, D.K. Arnett, M.J. Blaha, M. Cushman, S.R. Das, S. de Ferranti, J.P. Despres, H.J. Fullerton, V.J. Howard, M.D. Huffman, C.R. Isasi, M.C. Jimenez, S.E. Judd, B.M. Kissela, J.H. Lichtman, L.D. Lisabeth, S. Liu, R.H. Mackey, D.J. Magid, D.K. McGuire, E.R. Mohler, 3rd, C.S. Moy, P. Muntner, M.E. Mussolino, K. Nasir, R.W. Neumar, G. Nichol, L. Palaniappan, D.K. Pandey, M.J. Reeves, C.J. Rodriguez, W. Rosamond, P.D. Sorlie, J. Stein, A. Towfighi, T.N. Turan, S.S. Virani, D. Woo, R.W. Yeh, M.B. Turner, Executive Summary: Heart Disease and Stroke Statistics--2016 Update: A Report From the American Heart Association, Circulation 133(4) (2016) 447-54.

[37] P.A. Heidenreich, J.G. Trogdon, O.A. Khavjou, J. Butler, K. Dracup, M.D. Ezekowitz, E.A. Finkelstein, Y. Hong, S.C. Johnston, A. Khera, D.M. Lloyd-Jones, S.A. Nelson, G. Nichol, D. Orenstein, P.W. Wilson, Y.J. Woo, Forecasting the future of cardiovascular

disease in the United States: a policy statement from the American Heart Association, Circulation 123(8) (2011) 933-44.

[38] G.K. Hansson, Inflammation, atherosclerosis, and coronary artery disease, N Engl J Med 352(16) (2005) 1685-95.

[39] S. Lewington, G. Whitlock, R. Clarke, P. Sherliker, J. Emberson, J. Halsey, N. Qizilbash, R. Peto, R. Collins, Blood cholesterol and vascular mortality by age, sex, and blood pressure: a meta-analysis of individual data from 61 prospective studies with 55,000 vascular deaths, Lancet 370(9602) (2007) 1829-39.

[40] B.V. Howard, D.C. Robbins, M.L. Sievers, E.T. Lee, D. Rhoades, R.B. Devereux, L.D. Cowan, R.S. Gray, T.K. Welty, O.T. Go, W.J. Howard, LDL cholesterol as a strong predictor of coronary heart disease in diabetic individuals with insulin resistance and low LDL: The Strong Heart Study, Arterioscler Thromb Vasc Biol 20(3) (2000) 830-5.

[41] P. Sun, K.M. Dwyer, C.N. Merz, W. Sun, C.A. Johnson, A.M. Shircore, J.H. Dwyer, Blood pressure, LDL cholesterol, and intima-media thickness: a test of the "response to injury" hypothesis of atherosclerosis, Arterioscler Thromb Vasc Biol 20(8) (2000) 2005-10.

[42] J. Davignon, P. Ganz, Role of endothelial dysfunction in atherosclerosis, Circulation 109(23 Suppl 1) (2004) III27-32.

[43] N.A. Shirwany, M.H. Zou, Arterial stiffness: a brief review, Acta Pharmacol Sin 31(10) (2010) 1267-76.

[44] W.C. Morgan, H.L. Hodge, Diagnostic evaluation of dyspnea, Am Fam Physician 57(4) (1998) 711-6.

[45] J.M. Schussler, Effectiveness and safety of transradial artery access for cardiac catheterization, Proc (Bayl Univ Med Cent) 24(3) (2011) 205-9.

[46] D.G. Katritsis, J.P. Ioannidis, Percutaneous coronary intervention versus conservative therapy in nonacute coronary artery disease: a meta-analysis, Circulation 111(22) (2005) 2906-12.

[47] J.W. Jukema, J.J. Verschuren, T.A. Ahmed, P.H. Quax, Restenosis after PCI. Part 1: pathophysiology and risk factors, Nat Rev Cardiol 9(1) (2011) 53-62.

[48] V. Farooq, B.D. Gogas, P.W. Serruys, Restenosis: delineating the numerous causes of drug-eluting stent restenosis, Circ Cardiovasc Interv 4(2) (2011) 195-205.

[49] G.D. Dangas, B.E. Claessen, A. Caixeta, E.A. Sanidas, G.S. Mintz, R. Mehran, In-stent restenosis in the drug-eluting stent era, J Am Coll Cardiol 56(23) (2010) 1897-907.

[50] J.M. Bourget, R. Gauvin, D. Larouche, A. Lavoie, R. Labbe, F.A. Auger, L. Germain, Human fibroblast-derived ECM as a scaffold for vascular tissue engineering, Biomaterials 33(36) (2012) 9205-9213.

[51] A.R. Halabi, J.H. Alexander, L.K. Shaw, T.J. Lorenz, L. Liao, D.F. Kong, C.A. Milano, R.A. Harrington, P.K. Smith, Relation of early saphenous vein graft failure to outcomes following coronary artery bypass surgery, Am J Cardiol 96(9) (2005) 1254-9.

[52] P.W. Serruys, M.C. Morice, A.P. Kappetein, A. Colombo, D.R. Holmes, M.J. Mack, E. Stahle, T.E. Feldman, M. van den Brand, E.J. Bass, N. Van Dyck, K. Leadley, K.D. Dawkins, F.W. Mohr, Percutaneous coronary intervention versus coronary-artery bypass grafting for severe coronary artery disease, N Engl J Med 360(10) (2009) 961-72.

[53] M. Lovett, K. Lee, A. Edwards, D.L. Kaplan, Vascularization strategies for tissue engineering, Tissue Eng Part B Rev 15(3) (2009) 353-70.

[54] S.H. Ku, C.B. Park, Human endothelial cell growth on mussel-inspired nanofiber scaffold for vascular tissue engineering, Biomaterials 31(36) (2010) 9431-7.

[55] I.L. Geenen, D.G. Molin, N.M. van den Akker, F. Jeukens, H.M. Spronk, G.W. Schurink, M.J. Post, Endothelial cells (ECs) for vascular tissue engineering: venous ECs are less thrombogenic than arterial ECs, J Tissue Eng Regen Med 9(5) (2015) 564-76.

[56] X. Chen, A.S. Aledia, S.A. Popson, L. Him, C.C. Hughes, S.C. George, Rapid anastomosis of endothelial progenitor cell-derived vessels with host vasculature is promoted by a high density of cotransplanted fibroblasts, Tissue Eng Part A 16(2) (2010) 585-94.

[57] M. Olausson, V.K. Kuna, G. Travnikova, H. Backdahl, P.B. Patil, R. Saalman, H. Borg, A. Jeppsson, S. Sumitran-Holgersson, In Vivo Application of Tissue-Engineered Veins Using Autologous Peripheral Whole Blood: A Proof of Concept Study, EBioMedicine 1(1) (2014) 72-9.

[58] J.D. Roh, R. Sawh-Martinez, M.P. Brennan, S.M. Jay, L. Devine, D.A. Rao, T. Yi, T.L. Mirensky, A. Nalbandian, B. Udelsman, N. Hibino, T. Shinoka, W.M. Saltzman, E. Snyder, T.R. Kyriakides, J.S. Pober, C.K. Breuer, Tissue-engineered vascular grafts transform into mature blood vessels via an inflammation-mediated process of vascular remodeling, Proc Natl Acad Sci U S A 107(10) (2010) 4669-74.

[59] T.F. Whayne, A review of the role of anticoagulation in the treatment of peripheral arterial disease, Int J Angiol 21(4) (2012) 187-94.

[60] Y. Wang, J. Hu, J. Jiao, Z. Liu, Z. Zhou, C. Zhao, L.J. Chang, Y.E. Chen, P.X. Ma, B. Yang, Engineering vascular tissue with functional smooth muscle cells derived from human iPS cells and nanofibrous scaffolds, Biomaterials 35(32) (2014) 8960-9.

[61] V.K. Bajpai, S.T. Andreadis, Stem cell sources for vascular tissue engineering and regeneration, Tissue Eng Part B Rev 18(5) (2012) 405-25.

[62] P. Au, J. Tam, D. Fukumura, R.K. Jain, Bone marrow-derived mesenchymal stem cells facilitate engineering of long-lasting functional vasculature, Blood 111(9) (2008) 4551-8.

[63] N.F. Huang, S. Li, Mesenchymal stem cells for vascular regeneration, Regen Med 3(6) (2008) 877-92.

[64] C.A. Herberts, M.S. Kwa, H.P. Hermsen, Risk factors in the development of stem cell therapy, J Transl Med 9 (2011) 29.

[65] C. Xie, R.P. Ritchie, H. Huang, J. Zhang, Y.E. Chen, Smooth muscle cell differentiation in vitro: models and underlying molecular mechanisms, Arterioscler Thromb Vasc Biol 31(7) (2011) 1485-94.

[66] Z. Gong, L.E. Niklason, Use of human mesenchymal stem cells as alternative source of smooth muscle cells in vessel engineering, Methods Mol Biol 698 (2011) 279-94.

[67] S. Sundaram, L.E. Niklason, Smooth muscle and other cell sources for human blood vessel engineering, Cells Tissues Organs 195(1-2) (2012) 15-25.

[68] P.S. McFetridge, K. Abe, M. Horrocks, J.B. Chaudhuri, Vascular tissue engineering: bioreactor design considerations for extended culture of primary human vascular smooth muscle cells, ASAIO J 53(5) (2007) 623-30.

[69] E.S. Place, N.D. Evans, M.M. Stevens, Complexity in biomaterials for tissue engineering, Nat Mater 8(6) (2009) 457-70.

[70] J.P. Stegemann, S.N. Kaszuba, S.L. Rowe, Review: advances in vascular tissue engineering using protein-based biomaterials, Tissue Eng 13(11) (2007) 2601-13.

[71] C.J. Dong, Y.G. Lv, Application of Collagen Scaffold in Tissue Engineering: Recent Advances and New Perspectives, Polymers-Basel 8(2) (2016).

[72] X. Wang, W. Zhai, C. Wu, B. Ma, J. Zhang, H. Zhang, Z. Zhu, J. Chang, Procyanidins-crosslinked aortic elastin scaffolds with distinctive anti-calcification and biological properties, Acta Biomater 16 (2015) 81-93.

[73] S.L.M. Dahl, J.L. Blum, L.E. Niklason, Bioengineered Vascular Grafts: Can We Make Them Off-the-Shelf?, Trends Cardiovas Med 21(3) (2011) 83-89.

[74] S. Ravi, E.L. Chaikof, Biomaterials for vascular tissue engineering, Regen Med 5(1) (2010) 107-20.

[75] K.A. Rocco, M.W. Maxfield, C.A. Best, E.W. Dean, C.K. Breuer, In vivo applications of electrospun tissue-engineered vascular grafts: a review, Tissue Eng Part B Rev 20(6) (2014) 628-40.

[76] T.J. Sill, H.A. von Recum, Electrospinning: applications in drug delivery and tissue engineering, Biomaterials 29(13) (2008) 1989-2006.

[77] I.M. El-Sherbiny, M.H. Yacoub, Hydrogel scaffolds for tissue engineering: Progress and challenges, Glob Cardiol Sci Pract 2013(3) (2013) 316-42.

[78] J. Zhu, R.E. Marchant, Design properties of hydrogel tissue-engineering scaffolds, Expert Rev Med Devices 8(5) (2011) 607-26.

[79] J. Liu, H. Zheng, P.S. Poh, H.G. Machens, A.F. Schilling, Hydrogels for Engineering of Perfusable Vascular Networks, Int J Mol Sci 16(7) (2015) 15997-6016.

[80] N. Annabi, J.W. Nichol, X. Zhong, C. Ji, S. Koshy, A. Khademhosseini, F. Dehghani, Controlling the porosity and microarchitecture of hydrogels for tissue engineering, Tissue Eng Part B Rev 16(4) (2010) 371-83.

[81] F. Intranuovo, R. Gristina, F. Brun, S. Mohammadi, G. Ceccone, E. Sardella, F. Rossi, G. Tromba, P. Favia, Plasma Modification of PCL Porous Scaffolds Fabricated by Solvent-Casting/ParticulateLeaching for Tissue Engineering, Plasma Process Polym 11(2) (2014) 184-195.

[82] L. Song, Q. Zhou, P. Duan, P. Guo, D. Li, Y. Xu, S. Li, F. Luo, Z. Zhang, Successful development of small diameter tissue-engineering vascular vessels by our novel integrally designed pulsatile perfusion-based bioreactor, PLoS One 7(8) (2012) e42569.

[83] S.I. Jeong, J.H. Kwon, J.I. Lim, S.W. Cho, Y. Jung, W.J. Sung, S.H. Kim, Y.H. Kim, Y.M. Lee, B.S. Kim, C.Y. Choi, S.J. Kim, Mechano-active tissue engineering of vascular smooth muscle using pulsatile perfusion bioreactors and elastic PLCL scaffolds, Biomaterials 26(12) (2005) 1405-11.

[84] I. Martin, D. Wendt, M. Heberer, The role of bioreactors in tissue engineering, Trends Biotechnol 22(2) (2004) 80-6.

[85] S.I. Jeong, S.Y. Kim, S.K. Cho, M.S. Chong, K.S. Kim, H. Kim, S.B. Lee, Y.M. Lee, Tissue-engineered vascular grafts composed of marine collagen and PLGA fibers using pulsatile perfusion bioreactors, Biomaterials 28(6) (2007) 1115-22.

[86] M. Lovett, G. Eng, J.A. Kluge, C. Cannizzaro, G. Vunjak-Novakovic, D.L. Kaplan, Tubular silk scaffolds for small diameter vascular grafts, Organogenesis 6(4) (2010) 217-24.

[87] D.G. Seifu, A. Purnama, K. Mequanint, D. Mantovani, Small-diameter vascular tissue engineering, Nat Rev Cardiol 10(7) (2013) 410-21.

[88] D. Pankajakshan, D.K. Agrawal, Scaffolds in tissue engineering of blood vessels, Can J Physiol Pharmacol 88(9) (2010) 855-73.

[89] F. Loth, P.F. Fischer, H.S. Bassiouny, Blood flow in end-to-side anastomoses, Annu Rev Fluid Mech 40 (2008) 367-393.

[90] A.G. Mikos, S.W. Herring, P. Ochareon, J. Elisseeff, H.H. Lu, R. Kandel, F.J. Schoen, M. Toner, D. Mooney, A. Atala, M.E. Van Dyke, D. Kaplan, G. Vunjak-Novakovic, Engineering complex tissues, Tissue Eng 12(12) (2006) 3307-39.

[91] A. Kurane, N. Vyavahare, In vivo vascular tissue engineering: influence of cytokine and implant location on tissue specific cellular recruitment, J Tissue Eng Regen Med 3(4) (2009) 280-9.

[92] K.W. Lee, D.B. Stolz, Y. Wang, Substantial expression of mature elastin in arterial constructs, Proc Natl Acad Sci U S A 108(7) (2011) 2705-10.

[93] J.P. Stegemann, H. Hong, R.M. Nerem, Mechanical, biochemical, and extracellular matrix effects on vascular smooth muscle cell phenotype, J Appl Physiol (1985) 98(6) (2005) 2321-7.

[94] O. Benzakour, C. Kanthou, S.M. Kanse, M.F. Scully, V.V. Kakkar, D.N. Cooper, Evidence for cultured human vascular smooth muscle cell heterogeneity: isolation of clonal cells and study of their growth characteristics, Thromb Haemost 75(5) (1996) 854-8.

[95] D.E. Muylaert, J.O. Fledderus, C.V. Bouten, P.Y. Dankers, M.C. Verhaar, Combining tissue repair and tissue engineering; bioactivating implantable cell-free vascular scaffolds, Heart 100(23) (2014) 1825-30.

[96] S. Tara, H. Kurobe, M.W. Maxfield, K.A. Rocco, T. Yi, Y. Naito, C.K. Breuer, T. Shinoka, Evaluation of remodeling process in small-diameter cell-free tissue-engineered arterial graft, J Vasc Surg 62(3) (2015) 734-43.

[97] M.J. Zhang, Y. Zhou, L. Chen, Y.Q. Wang, X. Wang, Y. Pi, C.Y. Gao, J.C. Li, L.L. Zhang, An overview of potential molecular mechanisms involved in VSMC phenotypic modulation, Histochem Cell Biol 145(2) (2016) 119-30.

[98] M.G. Frid, B.V. Shekhonin, V.E. Koteliansky, M.A. Glukhova, Phenotypic changes of human smooth muscle cells during development: late expression of heavy caldesmon and calponin, Dev Biol 153(2) (1992) 185-93.

[99] S. Chang, S. Song, J. Lee, J. Yoon, J. Park, S. Choi, J.K. Park, K. Choi, C. Choi, Phenotypic modulation of primary vascular smooth muscle cells by short-term culture on micropatterned substrate, PLoS One 9(2) (2014) e88089.

[100] G. Wang, L. Jacquet, E. Karamariti, Q. Xu, Origin and differentiation of vascular smooth muscle cells, J Physiol 593(14) (2015) 3013-30.

[101] J.A. Beamish, P. He, K. Kottke-Marchant, R.E. Marchant, Molecular regulation of contractile smooth muscle cell phenotype: implications for vascular tissue engineering, Tissue Eng Part B Rev 16(5) (2010) 467-91.

[102] N.F. Worth, B.E. Rolfe, J. Song, G.R. Campbell, Vascular smooth muscle cell phenotypic modulation in culture is associated with reorganisation of contractile and cytoskeletal proteins, Cell Motil Cytoskeleton 49(3) (2001) 130-45.

[103] E.M. Rzucidlo, K.A. Martin, R.J. Powell, Regulation of vascular smooth muscle cell differentiation, J Vasc Surg 45 Suppl A (2007) A25-32.

[104] G.K. Owens, M.S. Kumar, B.R. Wamhoff, Molecular regulation of vascular smooth muscle cell differentiation in development and disease, Physiol Rev 84(3) (2004) 767-801.

[105] S.S. Rensen, P.A. Doevendans, G.J. van Eys, Regulation and characteristics of vascular smooth muscle cell phenotypic diversity, Neth Heart J 15(3) (2007) 100-8.

[106] S.R. Peyton, C.B. Raub, V.P. Keschrumrus, A.J. Putnam, The use of poly(ethylene glycol) hydrogels to investigate the impact of ECM chemistry and mechanics on smooth muscle cells, Biomaterials 27(28) (2006) 4881-93.

[107] S.B.H. Timraz, R. Rezgui, S.M. Boularaoui, J.C.M. Teo, Stiffness of Extracellular Matrix Components Modulates the Phenotype of Human Smooth Muscle Cells in Vitro and Allows for the Control of Properties of Engineered Tissues, Procedia Engineer 110 (2015) 29-36.

[108] S.R. Peyton, P.D. Kim, C.M. Ghajar, D. Seliktar, A.J. Putnam, The effects of matrix stiffness and RhoA on the phenotypic plasticity of smooth muscle cells in a 3-D biosynthetic hydrogel system, Biomaterials 29(17) (2008) 2597-607.

[109] R.J. Petrie, K.M. Yamada, At the leading edge of three-dimensional cell migration, J Cell Sci 125(Pt 24) (2012) 5917-26.

[110] H. Hong, J.P. Stegemann, 2D and 3D collagen and fibrin biopolymers promote specific ECM and integrin gene expression by vascular smooth muscle cells, J Biomater Sci Polym Ed 19(10) (2008) 1279-93.

[111] S. Lin, M. Sandig, K. Mequanint, Three-dimensional topography of synthetic scaffolds induces elastin synthesis by human coronary artery smooth muscle cells, Tissue Eng Part A 17(11-12) (2011) 1561-71.

[112] M. Rhinn, P. Dolle, Retinoic acid signalling during development, Development 139(5) (2012) 843-58.

[113] J.M. Miano, B.C. Berk, Retinoids: versatile biological response modifiers of vascular smooth muscle phenotype, Circ Res 87(5) (2000) 355-62.

[114] Y.R. Zhang, Y.Q. Zhao, J.F. Huang, Retinoid-binding proteins: similar protein architectures bind similar ligands via completely different ways, PLoS One 7(5) (2012) e36772.

[115] R.K. Kam, Y. Deng, Y. Chen, H. Zhao, Retinoic acid synthesis and functions in early embryonic development, Cell Biosci 2(1) (2012) 11.

[116] D. Dong, S.E. Ruuska, D.J. Levinthal, N. Noy, Distinct roles for cellular retinoic acid-binding proteins I and II in regulating signaling by retinoic acid, J Biol Chem 274(34) (1999) 23695-8.

[117] P. Germain, P. Chambon, G. Eichele, R.M. Evans, M.A. Lazar, M. Leid, A.R. De Lera, R. Lotan, D.J. Mangelsdorf, H. Gronemeyer, International Union of Pharmacology. LX. Retinoic acid receptors, Pharmacol Rev 58(4) (2006) 712-25.

[118] P. Neuville, Z. Yan, A. Gidlof, M.S. Pepper, G.K. Hansson, G. Gabbiani, A. Sirsjo, Retinoic acid regulates arterial smooth muscle cell proliferation and phenotypic features in vivo and in vitro through an RARalpha-dependent signaling pathway, Arterioscler Thromb Vasc Biol 19(6) (1999) 1430-6.

[119] D.I. Axel, A. Frigge, J. Dittmann, H. Runge, I. Spyridopoulos, R. Riessen, R. Viebahn, K.R. Karsch, All-trans retinoic acid regulates proliferation, migration, differentiation, and extracellular matrix turnover of human arterial smooth muscle cells, Cardiovasc Res 49(4) (2001) 851-62.

[120] H. Ou, J. Haendeler, M.R. Aebly, L.A. Kelly, B.C. Cholewa, G. Koike, A. Kwitek-Black, H.J. Jacob, B.C. Berk, J.M. Miano, Retinoic acid-induced tissue transglutaminase and apoptosis in vascular smooth muscle cells, Circ Res 87(10) (2000) 881-7.

[121] B. Zheng, M. Han, J.K. Wen, Role of Kruppel-like factor 4 in phenotypic switching and proliferation of vascular smooth muscle cells, IUBMB Life 62(2) (2010) 132-9.

[122] M.V. Autieri, Kruppel-like factor 4: transcriptional regulator of proliferation, or inflammation, or differentiation, or all three?, Circ Res 102(12) (2008) 1455-7.

[123] C. Wang, M. Han, X.M. Zhao, J.K. Wen, Kruppel-like factor 4 is required for the expression of vascular smooth muscle cell differentiation marker genes induced by all-trans retinoic acid, J Biochem 144(3) (2008) 313-21.

[124] H. Haller, C. Lindschau, P. Quass, A. Distler, F.C. Luft, Differentiation of vascular smooth muscle cells and the regulation of protein kinase C-alpha, Circ Res 76(1) (1995) 21-9.

[125] K. Tran-Lundmark, P. Tannenberg, B.H. Rauch, J. Ekstrand, P.K. Tran, U. Hedin, M.G. Kinsella, Perlecan Heparan Sulfate Is Required for the Inhibition of Smooth Muscle Cell Proliferation by All-trans-Retinoic Acid, J Cell Physiol 230(2) (2015) 482-7.

[126] A. Orlandi, S. Pucci, A. Ciucci, F. Pichiorri, A. Ferlosio, L.G. Spagnoli, Modulation of clusterin isoforms is associated with all-trans retinoic acid-induced proliferative arrest and apoptosis of intimal smooth muscle cells, Arterioscler Thromb Vasc Biol 25(2) (2005) 348-53.

[127] S. Tajima, A. Hayashi, T. Suzuki, Elastin expression is up-regulated by retinoic acid but not by retinol in chick embryonic skin fibroblasts, J Dermatol Sci 15(3) (1997) 166-72.

[128] J.T. Mao, J.G. Goldin, J. Dermand, G. Ibrahim, M.S. Brown, A. Emerick, M.F. McNitt-Gray, D.W. Gjertson, F. Estrada, D.P. Tashkin, M.D. Roth, A pilot study of all-trans-retinoic acid for the treatment of human emphysema, Am J Respir Crit Care Med 165(5) (2002) 718-23.

[129] G.J. Fisher, J.J. Voorhees, Molecular mechanisms of retinoid actions in skin, FASEB J 10(9) (1996) 1002-13.

[130] B. Liu, C.S. Harvey, S.E. McGowan, Retinoic acid increases elastin in neonatal rat lung fibroblast cultures, Am J Physiol 265(5 Pt 1) (1993) L430-7.

[131] S. McGowan, S.K. Jackson, M. Jenkins-Moore, H.H. Dai, P. Chambon, J.M. Snyder, Mice bearing deletions of retinoic acid receptors demonstrate reduced lung elastin and alveolar numbers, Am J Respir Cell Mol Biol 23(2) (2000) 162-7.

[132] Y. Liu, H. Chen, D. Mu, D. Li, Y. Zhong, N. Jiang, Y. Zhang, M. Xia, Association of Serum Retinoic Acid With Risk of Mortality in Patients With Coronary Artery Disease, Circ Res 119(4) (2016) 557-63.

[133] A. Hayashi, T. Suzuki, S. Tajima, Modulations of elastin expression and cell proliferation by retinoids in cultured vascular smooth muscle cells, J Biochem 117(1) (1995) 132-6.

[134] L.M. Barone, B. Faris, S.D. Chipman, P. Toselli, B.W. Oakes, C. Franzblau, Alteration of the extracellular matrix of smooth muscle cells by ascorbate treatment, Biochim Biophys Acta 840(2) (1985) 245-54.

[135] M. Chojkier, K. Houglum, J. Solis-Herruzo, D.A. Brenner, Stimulation of collagen gene expression by ascorbic acid in cultured human fibroblasts. A role for lipid peroxidation?, J Biol Chem 264(28) (1989) 16957-62.

[136] H. Qiao, J. Bell, S. Juliao, L. Li, J.M. May, Ascorbic acid uptake and regulation of type I collagen synthesis in cultured vascular smooth muscle cells, J Vasc Res 46(1) (2009) 15-24.

[137] J.M. Davidson, P.A. LuValle, O. Zoia, D. Quaglino, Jr., M. Giro, Ascorbate differentially regulates elastin and collagen biosynthesis in vascular smooth muscle cells and skin fibroblasts by pretranslational mechanisms, J Biol Chem 272(1) (1997) 345-52.

[138] B.M. Ogle, D.L. Mooradian, Manipulation of remodeling pathways to enhance the mechanical properties of a tissue engineered blood vessel, J Biomech Eng 124(6) (2002) 724-33.

[139] S. Grenier, M. Sandig, K. Mequanint, Polyurethane biomaterials for fabricating 3D porous scaffolds and supporting vascular cells, J Biomed Mater Res A 82(4) (2007) 802-9.

[140] Z. Urban, O. Agapova, V. Hucthagowder, P. Yang, B.C. Starcher, M.R. Hernandez, Population differences in elastin maturation in optic nerve head tissue and astrocytes, Invest Ophthalmol Vis Sci 48(7) (2007) 3209-15.

[141] X. Wu, Y. Zou, Q. Zhou, L. Huang, H. Gong, A. Sun, K. Tateno, K. Katsube, F. Radtke, J. Ge, T. Minamino, I. Komuro, Role of Jagged1 in arterial lesions after vascular injury, Arterioscler Thromb Vasc Biol 31(9) (2011) 2000-6.

[142] X. Wang, T. Lou, W. Zhao, G. Song, C. Li, G. Cui, The effect of fiber size and pore size on cell proliferation and infiltration in PLLA scaffolds on bone tissue engineering, J Biomater Appl 30(10) (2016) 1545-51.

[143] L. Olah, K. Filipczak, Z. Jaegermann, T. Czigany, L. Borbas, S. Sosnowski, P. Ulanski, J.M. Rosiak, Synthesis, structural and mechanical properties of porous polymeric scaffolds for bone tissue regeneration based on neat poly(epsilon-caprolactone) calcium carbonate, Polym Advan Technol 17(11-12) (2006) 889-897.

[144] M.A. Woodruff, D.W. Hutmacher, The return of a forgotten polymer-Polycaprolactone in the 21st century, Prog Polym Sci 35(10) (2010) 1217-1256.

[145] B.D. Ulery, L.S. Nair, C.T. Laurencin, Biomedical Applications of Biodegradable Polymers, J Polym Sci Pol Phys 49(12) (2011) 832-864.

[146] Y. Hong, J. Guan, K.L. Fujimoto, R. Hashizume, A.L. Pelinescu, W.R. Wagner, Tailoring the degradation kinetics of poly(ester carbonate urethane)urea thermoplastic elastomers for tissue engineering scaffolds, Biomaterials 31(15) (2010) 4249-58.

[147] Q. Jiang, H. Xu, S. Cai, Y. Yang, Ultrafine fibrous gelatin scaffolds with deep cell infiltration mimicking 3D ECMs for soft tissue repair, J Mater Sci Mater Med 25(7) (2014) 1789-800.

[148] M.T. Nelson, L. Pattanaik, M. Allen, M. Gerbich, K. Hux, J.J. Lannutti, Recrystallization improves the mechanical properties of sintered electrospun polycaprolactone, J Mech Behav Biomed Mater 30 (2014) 150-8.

[149] S. Lin, K. Mequanint, The role of Ras-ERK-IL-1beta signaling pathway in upregulation of elastin expression by human coronary artery smooth muscle cells cultured in 3D scaffolds, Biomaterials 33(29) (2012) 7047-56.

[150] P.J. Woodward, D.H. Merino, B.W. Greenland, I.W. Hamley, Z. Light, A.T. Slark, W. Hayes, Hydrogen Bonded Supramolecular Elastomers: Correlating Hydrogen Bonding Strength with Morphology and Rheology, Macromolecules 43(5) (2010) 2512-2517.

[151] Z. Tosun, P.S. McFetridge, Improved recellularization of ex vivo vascular scaffolds using directed transport gradients to modulate ECM remodeling, Biotechnol Bioeng 110(7) (2013) 2035-2045.

[152] P. Losi, S. Lombardi, E. Briganti, G. Soldani, Luminal surface microgeometry affects platelet adhesion in small-diameter synthetic grafts, Biomaterials 25(18) (2004) 4447-55.

[153] Z.G. Tang, R.A. Black, J.M. Curran, J.A. Hunt, N.P. Rhodes, D.F. Williams, Surface properties and biocompatibility of solvent-cast poly[-caprolactone] films, Biomaterials 25(19) (2004) 4741-8.

[154] B.H. Kim, D.H. Lee, J.Y. Kim, D.O. Shin, H.Y. Jeong, S. Hong, J.M. Yun, C.M. Koo, H. Lee, S.O. Kim, Mussel-inspired block copolymer lithography for low surface energy materials of teflon, graphene, and gold, Adv Mater 23(47) (2011) 5618-22.

[155] M. Choudhury, S. Mohanty, S. Nayak, Effect of Different Solvents in Solvent Casting of Porous PLA Scaffolds-In Biomedical and Tissue Engineering Applications, J Biomater Tiss Eng 5(1) (2015) 1-9.

[156] S. Bertoldi, S. Fare, M.C. Tanzi, Assessment of scaffold porosity: the new route of micro-CT, J Appl Biomater Biomech 9(3) (2011) 165-75.

[157] G. Lalwani, A. Gopalan, M. D'Agati, J.S. Sankaran, S. Judex, Y.X. Qin, B. Sitharaman, Porous three-dimensional carbon nanotube scaffolds for tissue engineering, J Biomed Mater Res A 103(10) (2015) 3212-25.

[158] S. Grenier, M. Sandig, D.W. Holdsworth, K. Mequanint, Interactions of coronary artery smooth muscle cells with 3D porous polyurethane scaffolds, J Biomed Mater Res A 89(2) (2009) 293-303.

[159] H.Y. Oh, X. Jin, J.G. Kim, M.J. Oh, X. Pian, J.M. Kim, M.S. Yoon, C.I. Son, Y.S. Lee, K.C. Hong, H. Kim, Y.J. Choi, K.Y. Whang, Characteristics of primary and immortalized fibroblast cells derived from the miniature and domestic pigs, BMC Cell Biol 8 (2007) 20.

[160] J.P. Mazzoccoli, D.L. Feke, H. Baskaran, P.N. Pintauro, Mechanical and cell viability properties of crosslinked low- and high-molecular weight poly(ethylene glycol) diacrylate blends, J Biomed Mater Res A 93(2) (2010) 558-66.

[161] G.D. Nicodemus, S.J. Bryant, Cell encapsulation in biodegradable hydrogels for tissue engineering applications, Tissue Eng Part B Rev 14(2) (2008) 149-65.

[162] T. Hodgkinson, X.F. Yuan, A. Bayat, Electrospun silk fibroin fiber diameter influences in vitro dermal fibroblast behavior and promotes healing of ex vivo wound models, J Tissue Eng 5 (2014) 2041731414551661.

[163] V.M. Quent, D. Loessner, T. Friis, J.C. Reichert, D.W. Hutmacher, Discrepancies between metabolic activity and DNA content as tool to assess cell proliferation in cancer research, J Cell Mol Med 14(4) (2010) 1003-13.

[164] S. Patel, Y. Shi, R. Niculescu, E.H. Chung, J.L. Martin, A. Zalewski, Characteristics of coronary smooth muscle cells and adventitial fibroblasts, Circulation 101(5) (2000) 524-32.

[165] A. Bhattacharyya, S. Lin, M. Sandig, K. Mequanint, Regulation of vascular smooth muscle cell phenotype in three-dimensional coculture system by Jagged1-selective Notch3 signaling, Tissue Eng Part A 20(7-8) (2014) 1175-87.

[166] S. Grenier, M. Sandig, K. Mequanint, Smooth muscle alpha-actin and calponin expression and extracellular matrix production of human coronary artery smooth muscle cells in 3D scaffolds, Tissue Eng Part A 15(10) (2009) 3001-11.

[167] T. Steynberg, M. Visagie, T. Mqoco, A. Idicula, S. Moolman, W. Richter, A. Joubert, Qualitative assessment of smooth muscle cells propagated on 2D-and 3D-polycaprolactone polymers via scanning electron microscope., Biomed Res-India 23(2) (2012) 191-198.

[168] R. Pankov, K.M. Yamada, Fibronectin at a glance, J Cell Sci 115(Pt 20) (2002) 3861-3.

[169] G. Dubey, K. Mequanint, Conjugation of fibronectin onto three-dimensional porous scaffolds for vascular tissue engineering applications, Acta Biomater 7(3) (2011) 1114-25.

[170] A. Tiwari, A. Kidane, H. Salacinski, G. Punshon, G. Hamilton, A.M. Seifalian, Improving endothelial cell retention for single stage seeding of prosthetic grafts: use of polymer sequences of arginine-glycine-aspartate, Eur J Vasc Endovasc Surg 25(4) (2003) 325-9.

[171] G.A. Villalona, B. Udelsman, D.R. Duncan, E. McGillicuddy, R.F. Sawh-Martinez, N. Hibino, C. Painter, T. Mirensky, B. Erickson, T. Shinoka, C.K. Breuer, Cell-seeding techniques in vascular tissue engineering, Tissue Eng Part B Rev 16(3) (2010) 341-50.

[172] M.M. Medhora, Retinoic acid upregulates beta(1)-integrin in vascular smooth muscle cells and alters adhesion to fibronectin, Am J Physiol Heart Circ Physiol 279(1) (2000) H382-7.

[173] W.Y. Hu, N. Fukuda, C. Satoh, T. Jian, A. Kubo, M. Nakayama, H. Kishioka, K. Kanmatsuse, Phenotypic modulation by fibronectin enhances the angiotensin II-generating system in cultured vascular smooth muscle cells, Arterioscler Thromb Vasc Biol 20(6) (2000) 1500-5.

[174] L. Ades, A. Guerci, E. Raffoux, M. Sanz, P. Chevallier, S. Lapusan, C. Recher, X. Thomas, C. Rayon, S. Castaigne, O. Tournilhac, S. de Botton, N. Ifrah, J.Y. Cahn, E. Solary, C. Gardin, N. Fegeux, D. Bordessoule, A. Ferrant, S. Meyer-Monard, N. Vey, H. Dombret, L. Degos, S. Chevret, P. Fenaux, Very long-term outcome of acute

promyelocytic leukemia after treatment with all-trans retinoic acid and chemotherapy: the European APL Group experience, Blood 115(9) (2010) 1690-6.

[175] S. Wakino, U. Kintscher, S. Kim, S. Jackson, F. Yin, S. Nagpal, R.A. Chandraratna, W.A. Hsueh, R.E. Law, Retinoids inhibit proliferation of human coronary smooth muscle cells by modulating cell cycle regulators, Arterioscler Thromb Vasc Biol 21(5) (2001) 746-51.

[176] A.J. Michels, B. Frei, Myths, artifacts, and fatal flaws: identifying limitations and opportunities in vitamin C research, Nutrients 5(12) (2013) 5161-92.

[177] C.M. Shanahan, P.L. Weissberg, Smooth muscle cell heterogeneity: patterns of gene expression in vascular smooth muscle cells in vitro and in vivo, Arterioscler Thromb Vasc Biol 18(3) (1998) 333-8.

[178] A.J. Ryan, F.J. O'Brien, Insoluble elastin reduces collagen scaffold stiffness, improves viscoelastic properties, and induces a contractile phenotype in smooth muscle cells, Biomaterials 73 (2015) 296-307.

Appendix: Copyright Permission

Copyright Permissions for Figures that appeared in Chapter 2.

Figure 2.1

Obtained from Oxford University Press.

Figure 2.5

Obtained from Wolters Kluwer Health, Inc.

Curriculum Vitae

Brandon Chaffay

Education

2015-Present **MB BCh BAO Candidate**

University College Dublin School of Medicine, Ireland

2013-2016 **MESc. Chemical and Biochemical Engineering**

Western University, London, ON, Canada

2009-2013 **B.Sc. Life Sciences ssp. Microbiology & Immunology**

Queen's University, Kingston, ON, Canada

Related Work Experience

2014-2015 **Graduate Teaching Assistant**

Department of Chemical and Biochemical Engineering

Western University, London, ON, Canada